Noname manuscript No.
(will be inserted by the editor)

Cyclic negative feedback systems: what is the chance of oscillation?

Arnaud Tonnelier

the date of receipt and acceptance should be inserted later

Abstract Many biological oscillators have a cyclic structure consisting of negative feedback loops. In this paper, we analyze the impact that the addition of a positive or a negative self-feedback loop has on the oscillatory behavior of the three negative feedback oscillators proposed by Tsai et al. (Science 231:126-129, 2008) where, in contrast with numerous oscillator models, the interactions between elements occur via the modulation of the degradation rates. Through analytical and computational studies we show that an additional self-feedback affects the oscillatory behavior. In the high-cooperativity limit, i.e., for large Hill coefficients, we derive exact analytical conditions for oscillations and show that the relative location between the dissociation constants of the Hill functions and the ratio of kinetic parameters determines the possibility of oscillatory activities. We compute analytically the probability of oscillations for the three models and show that the smallest domain of periodic behavior is obtained for the negative-plus-negative feedback system whereas the additional positive self-feedback loop does not modify significantly the chance to oscillate. We numerically investigate to what extent the properties obtained in the sharp situation applied in the smooth case. Results suggest that a switch-like coupling behavior, a time-scale separation, and a repressilator-type architecture with an even number of elements facilitate the emergence of sustained oscillations in biological systems. An additional positive self-feedback loop produces robustness and adaptability whereas an additional negative self-feedback loop reduces the chance to oscillate.

Keywords Oscillation · Feedback · Limit cycle · Repressilator · Helmholtz decomposition

To the memory of José Manuel Zaldívar Comenges.

INRIA,
655 avenue de l'Europe, Montbonnot
38334 Saint Ismier, France
Tel.: +33-4-76615572
E-mail: arnaud.tonnelier@inria.fr

1 Introduction

Connected networks arising in systems biology show a wide variety of dynamical behaviors, oscillations being a recurrent motif. Oscillations frequently occur in the regulation of biological systems and play a fundamental role in numerous physiological processes as the hormone secretion (Walker et al. 2012), the cardiac electrical activity (Keener and Sneyd 1998), the circadian rhythm (Goldbeter 2002) or in pharmacodynamics (Dokoumetzidis et al. 2001), to mention a few. Therefore, an important topic in mathematical biology has been the study of necessary conditions for a system to show and maintain oscillations in a fluctuating environment such as the interior of a cell (Weber et al. 2011; Mincheva 2011; Tsai et al. 2008; Ferrell et al. 2011; and references therein).
It has been suggested that the dynamical properties of biological systems made of interacting elements could be understood in terms of network connectivity considering the so-called interaction graph (Thomas 1981; Kaufman et al. 2007; Mincheva 2011; Domijan and Pécou 2012; Purcell et al. 2010). A hallmark of robust oscillations is the existence of inhibitory feedback loops despite the fact that the occurrence of a negative feedback circuit is not necessary (Richard and Comet 2011). In addition, negative feedbacks are frequently embedded in a cyclic architecture (Fraser and Tiwari 1974; Hastings et al. 1977; Smith 1987; Mallet-Paret and Smith 1990; Goldbeter 1991; Elkhader 1992; Müller et al. 2006) that is believed to be the underlying circuit responsible for the emergence of oscillations in networks as in enzymatic reactions coupled with gene transcription (see references in (Hastings et al. 1977)), in cellular control systems, or in neural systems where the term 'ring' is used (see various examples and references in Sect. 4 of Mallet-Paret and Smith 1990). The repressilator is an archetypal instance of cyclic negative feedback system (Elowitz and Leibler 2000; Müller et al. 2006). This class of models has been extensively studied since the early work of Tyson (1975) which demonstrated the existence of large amplitude oscillations for a three-dimensional cyclic negative feedback system. Subsequently, several generalizations have been proposed and studied (Hastings 1977; Hastings et al. 1977; Smith 1986). It has been observed (Fraser and Tiwari, 1974) and proved (Smith 1987) that a qualitative difference occurs in the dynamics of negative cyclic systems between an odd number and an even number of nodes in the cycle. A significant insight has been accomplished in Mallet-Paret and Smith (1990) where it is shown that monotone cyclic feedback systems can be embedded in R^2 and, therefore, the possible dynamics of the network are severely constrained. In addition, common characteristics of global attractors for generic cyclic feedback systems have been described in (Gedeon and Mischaikow 1995; Gedeon 1998).
Even though negative feedback loops are enough to generate oscillations (Goldbeter 1991; Griffith 1968; Elowitz and Leibler 2000; Hirata et al. 2002; Tsai et al. 2008), many biological oscillators have also positive feedback loops (Harris and Levine 2005; Hornung and Barkai 2008; Angeli et al. 2004) raising the question of the functional role of these extra loops. Several explanations have

been proposed to justify the existence of positive loops in biological systems. A conjecture by Thomas (1981) demonstrated in (Snoussi 1998; Plahte et al. 1995; Gouzé 1998; Cinquin and Demongeot 2002) states that the presence of a positive feedback loop is a necessary condition for biological systems being able to possess multiple steady states. In particular, a bistable behavior inducing a switch-like response can be obtained (Angeli et al. 2004; Cherry and Adler 2000; Ferrell 2002). Tsai et al. (2008) argued that the existence of a positive feedback loop makes oscillatory systems easy to tune and more robust (see also Stricker et al. 2008). Other possible advantages include the reliability of oscillations, the noise-resistance of the system (Elowitz and Leibler 2000) and the stabilization of active states (López-Caamal et al. 2013). In addition, interaction of positive and negative loops are involved in the regulation of different physiological processes: the cell cycle (Goldbeter 2002), the generation of the well-known p53 oscillations (Ciliberto et al. 2005; Harris and Levine 2005) or the balance between noise buffering and signaling sensitivity (Hornung and Barkai 2008).

The study of the network architecture and its relation with the dynamical behavior has attracted a lot of attention but the geometrical properties of the vector field generating the flow of the system have been poorly explored. A first attempt in this direction has been carried out in (Demongeot et al. 2007a, 2007b) where it is shown that a close link exists between sustained oscillations and the existence of a potential-Hamiltonian decomposition of the vector field. However, the link with the interaction graph of the system and the applicability of the method to a dimension greater than two have not been addressed. There is a need to fill the gap between oscillations, interaction graph, and vector-field properties.

In this paper, we study the cyclic inhibitory feedback systems considered by Tsai et al. (2008) where the symmetry of the cycle can be broken by an additional negative or positive self-feedback loop. In Sect. 2 we present the models. In Sect. 3.1 we discuss the nature of the interactions and in Sect. 3.2 we exhibit a vector-field decomposition of the 3D system. Fixed points are studied in Sect. 3.3 and a qualitative description of oscillations in terms of slow-fast dynamics is provided (Sect. 3.4). In the idealized case of step-like coupling, we derive exact conditions for the existence of oscillations and we describe analytically the ranges of model parameter where stable limit cycles are found (Sect. 3.5). Numerical simulations in the smooth-coupling case are performed in Sect. 3.6. We generalize some results to large cyclic repression systems in Sect. 3.7 and we conclude by a discussion (Sect. 4).

2 Models

In this paper, we consider the oscillator models formulated in Tsai et al. (2008) (see also Angeli et al. 2004; Ferrell et al. 2011): the first oscillator model, referred to as the negative feedback-only oscillator (the No-oscillator in the sequel) is schematically illustrated in Fig. 1. If we denote by a, b and c, the

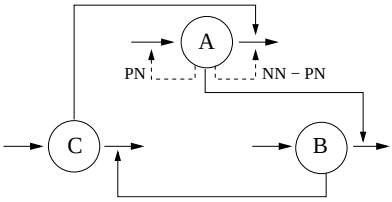

Fig. 1 Schematic view of the oscillator models. The additionnal loops of the negative-plus-negative oscillator (labelled NN) and positive-plus-negative oscillator (labelled PN) are represented in dotted lines.

concentration of the different molecules or chemical species (gene, protein, or metabolite), the equation for a reads

$$\frac{da}{dt} = \alpha_a - \beta_a a - \frac{\beta_{ac} a c^{n_c}}{K_c^{n_c} + c^{n_c}}$$

where it is assumed that the molecule is synthesized (or activated) at a constant rate α_a, degraded (or inactivated) at a rate β_a and the inhibition by another molecule (here c) is approximated by a Hill equation with $n_c > 0$ the Hill coefficient and $K_c > 0$ the median effective concentration value (or the half-maximal concentration). The rate constant β_{ac} determines the strength of inhibition of molecule a from molecule c. We assume that similar equations hold for b and c such that the system forms a cyclic negative feedback three-component oscillator. If we take

$$A = \frac{\beta_a a}{\alpha_a},\ k_1 = \beta_a,\ k_2 = \beta_{ac},\ K_1 = \frac{K_c \beta_c}{\alpha_c},\ and\ n_1 = n_c \tag{1}$$

(and similar change of variables for b and c) we end up with the dimensionless equations:

$$\begin{aligned} \frac{dA}{dt} &= k_1(1 - A) - k_2 A S_1(C), \\ \frac{dB}{dt} &= k_3(1 - B) - k_4 B S_2(A), \\ \frac{dC}{dt} &= k_5(1 - C) - k_6 C S_3(B), \end{aligned} \tag{2}$$

where $(k_i)_{i=1,\ldots,6} > 0$ are rate constants and $(S_i)_{i=1,2,3}$ are the Hill functions

$$S_i(x) = \frac{x^{n_i}}{K_i^{n_i} + x^{n_i}}. \tag{3}$$

Parameters K_i are also referred to as the microscopic dissociation constants or saturation constants, or when Hill functions exhibit a sharp transition, as thresholds or switching values. Without cooperative binding, i.e. for $n_i = 1$, the interactions follow the Michaelis-Menten kinetic model, K_i being the Michaelis constant.

Two other oscillators have been introduced: the negative-plus-negative oscillator (NN-oscillator in the sequel) and the positive-plus-negative oscillator (PN-oscillator in the sequel). These oscillators have an additional self-feedback loop on the A-component of the No-oscillator. For the NN-oscillator, Eq. (2) becomes

$$\frac{dA}{dt} = k_1(1 - A) - k_2 A S_1(C) - k_7 A S_4(A), \tag{4}$$

and for the PN-oscillator a positive feedback is introduced

$$\frac{dA}{dt} = k_1(1 - A) - k_2 A S_1(C) + k_7(1 - A) S_4(A), \tag{5}$$

where S_4 is given by (3). The No-oscillator belongs to the class of repressilator-type models (Elowitz and Leibler 2000) that are characterized by the cyclic inhibitory connection of elements (proteins that cyclically repress the synthesis of another). The presence of a positive self-feedback loop for the PN-oscillator is a characteristic feature of amplified negative feedback oscillators (Purcell et al. 2010) where one species amplifies its own production. It is worth noting that the coupling term can be rewritten as a modulation of the degradation rates unlike many regulatory models where the coupling acts on the synthesis term (we will discuss this point latter, section 3.5.2).
Due to the Bendixson's and Dulac's criteria, it is well known that the two components version of the No-oscillator and NN-oscillator are not able to generate oscillations and a minimal oscillator with negative interactions only has at least three components. The three-node architecture proposed for the No-oscillator model appears as a recurrent network motif in many different independent biological contexts (Pigolotti et al. 2007). It has been widely used as a generic and realistic minimal model responsible for the oscillatory behavior observed in complex networks (Goldbeter 1991; Ferrell et al. 2011; Boulier et al. 2007; Pigolotti et al. 2007).
Recently, a similar repressilator-type model has been studied in (Buse et al. 2009, 2010) where it has been shown that if the negative feedback is sufficiently strong and if the sigmoidal interaction is sufficiently stiff then the system oscillates. For the models studied here, it has been numerically observed by Tsai and coworkers (Tsai et al. 2008) that the three oscillator models exhibit oscillations and that oscillatory regimes are more easily obtained in the positive-plus-negative type oscillator whereas oscillations are limited by the negative self-feedback loop.

3 Results

3.1 The nature of interactions

The positive or negative nature of a loop is determined by the sign of the partial derivative of the functions involved in the loop and is commonly represented by

an interaction graph. The sign of the (i, j) component of the Jacobian matrix (see Appendix A), i.e., $\partial f_i/\partial x_j$, defines the nature of the connection from j to i and the product of the signs of the components occurring in the loop gives the nature of the feedback loop. In Tsai et al. (2008) another convention seems to be used since the sign of the scalar term describing the feedback in the equations determines the nature of the interaction. For the oscillators studied here the two definitions coincide except for the nature of the self-feedback loop of the PN-oscillator. The positive interaction term $(1 - A)S_4(A)$ in the PN-oscillator equation has a positive derivative on $(0, A^*)$ and a negative derivative on $(A^*, 1)$ where A^* is the unique solution of $x^{n_4+1}+(1+n_4)K_4^{n_4}x-n_4K_4^{n_4} = 0$. Adding the linear term $k_1(1 - A)$ the nature of the self-interaction remains variable and can become negative in particular when k_1 is sufficiently large. In the limit of large n_4 values, it is easy to show that the maximum of the derivative of the interaction term $(1 - A)S_4(A)$ is reached for $A = K_4$ (when $K_4 < 1$) and the feedback is non-negative if and only if

$$\frac{k_1}{k_7} < \frac{n_4}{4}\left(\frac{1}{K_4} - 1\right) - \frac{1}{2}$$

to a leading order in $1/n_4$. To sum up, the interactions between molecules induce a negative coupling. In addition, each molecule has a negative self-feedback loop describing the degradation but it is common to ignore it in the interaction graph (Fig. 1). The additional loop of the NN-oscillator does not change the nature of the self-feedback loop whereas for the PN-oscillator the nature of the loop becomes variable: it is negative when the degradation dominates and positive when amplification dominates. By abuse of language the PN-oscillator is referred to as an amplified negative feedback oscillator.
The oscillator models previously introduced can be generalized and written in an abstract form as

$$\frac{dx_i}{dt} = f_i(x_i, x_{i-1}), \quad i = 1, 2, \ldots, n$$

where we set $x_0 = x_n$ with n the number of species involved in the cycle. For the No-model we have

$$f_i(x_i, x_{i-1}) = k_{2i-1}(1 - x_i) - k_{2i}x_iS_i(x_{i-1}), \quad i = 1, 2, \ldots, n.$$

For the NN-model and PN-model an additional loop, that depends on x_1 only, is included in the definition of f_1 (see Eq.4, 5, respectively). It can be checked easely that $D = [0, 1]^n$ is positively invariant. Moreover, we have

$$\frac{\partial f_i(x_i, x_{i-1})}{\partial x_{i-1}} = -k_{2i}x_iS_i'(x_{i-1}) < 0, \quad \forall x \in D \text{ and } 1 \leq i \leq n$$

and therefore the different oscillators belong to the class of monotone cyclic feedback systems (Mallet-Paret and Smith 1990). It is worth noting that the models considered here do not satisfy the properties of the systems presented in (Hastings et al. 1977) and in (Smith 1987) and therefore previous theorems

on limit cycle existence do not apply here.
If we define u_i such that $x_i = e^{u_i}$, then the cyclic feedback system can be rewritten in a more standard decoupled form as

$$\frac{du_i}{dt} = a_i(u_i) - b_i(u_{i-1}), \quad i = 1, 2, \ldots, n$$

where $a_i(u) = k_{2i-1}(e^{-u} - 1)$ and $b_i(u) = k_{2i}S_i(e^u)$.

3.2 Helmholtz decomposition, energy dissipation and divergence

Oscillations in biological systems have been widely analyzed via the associated interaction graph but the geometrical properties of the system have been poorly addressed. One can expect that the structure of the vector field provides an intuitive understanding of the dynamics and gives some key elements to figure out the appearance of stable periodicity.
Let us define $S_k^{[1]}(x) = \int_0^x S_k(u)du$ and $S_k^{[2]}(x) = \int_0^x S_k^{[1]}(u)du$. Both integrals can be analytically expressed with the generalized hypergeometric functions ${}_pF_q(a_1, \ldots, a_p; b_1, \ldots, b_q; x)$ as

$$S_k^{[1]}(x) = x\big(1 -_2 F_1(1, 1/n_k; 1 + 1/n_k; -(x/K_k)^{n_k})\big), \tag{6}$$
$$S_k^{[2]}(x) = x\big(1 -_3 F_2(1, 1/n_k, 2/n_k; 1 + 2/n_k, 1 + 1/n_k; -(x/K_k)^{n_k})\big). \tag{7}$$

Let F_i be the vector field of oscillator i where $i \in \{\text{No, NN, PN}\}$ stands for one of the three different oscillators. The oscillators share a similar Helmholtz decomposition of their vector field

$$F_i = -\nabla\phi_i + \nabla \times G \tag{8}$$

where ϕ_i is a scalar potential defining the conservative part of the vector field. The vector potential G is identical for all oscillators and is given by

$$G(A, B, C) = \begin{pmatrix} k_6 C S_3^{[1]}(B) \\ k_2 A S_1^{[1]}(C) \\ k_4 B S_2^{[1]}(A) \end{pmatrix}.$$

The scalar potential ϕ_i can be decomposed as $\phi_i = \phi + \tilde{\phi}_i$ where ϕ is a potential common to all oscillators given by

$$\phi(A, B, C) = \frac{k_1}{2}(1 - A)^2 + k_4 S_2^{[2]}(A) + \frac{k_3}{2}(1 - B)^2 + k_6 S_3^{[2]}(B) + \\ + \frac{k_5}{2}(1 - C)^2 + k_2 S_1^{[2]}(C). \tag{9}$$

$\tilde{\phi}_i$ is an oscillator-dependent potential induced by the self-feedback loop and is given by

$$\begin{aligned}\tilde{\phi}_{No}(A) &= 0,\\ \tilde{\phi}_{NN}(A) &= k_7 A S_4^{[1]}(A) - k_7 S_4^{[2]}(A),\\ \tilde{\phi}_{PN}(A) &= k_7(A-1) S_4^{[1]}(A) - k_7 S_4^{[2]}(A).\end{aligned}$$

The vector field of each oscillator is the sum of a curl-free vector field, defined by ϕ_i, and a divergence-free vector field, defined by G. The divergence-free part defines the circulation density (source-free) of the oscillators and remains the same in the three versions of the oscillators. The curl-free part defines the source density and reflects the difference between each oscillator induced by the additional self-feedback. The modification of the source density term can be measured directly by the divergence of the vector field. Physically the divergence measures to which extent the flow generated by the vector field behaves as a source or a sink. The divergence describes the rate of change of an infinitesimal state space volume $V(t)$ following the flow defined by F and we have $\mathrm{div}(F(x)) = \dot{V}(t)/V(t)$. In conservative systems, there is no change of the total energy and therefore the state space volume is constant and $\mathrm{div}F = 0$. In non-conservative systems, if $\mathrm{div}F > 0$ the volume $V(t)$ increases and the vector-field flow behaves like a source, whereas if $\mathrm{div}F < 0$ then $V(t)$ decreases and the vector field flow behaves as a sink. We have

$$\mathrm{div}F_i = -\Delta\phi_i,$$

and we calculate for the No-oscillator

$$\mathrm{div}F_{No} = -k_1 - k_3 - k_5 - k_2 S_1(C) - k_4 S_2(A) - k_6 S_3(B) \tag{10}$$

which is negative. For the NN-oscillator, we get

$$\mathrm{div}F_{NN} = \mathrm{div}F_{No} - k_7 S_4(A) - k_7 A S_4'(A) \tag{11}$$

which is still negative. For the PN-oscillator, we obtain

$$\mathrm{div}F_{PN} = \mathrm{div}F_{No} - k_7 S_4(A) + k_7(1-A) S_4'(A) \tag{12}$$

which has $k_7(1-A)S_4'(A)$ as a positive term in the divergence showing the existence of a positive self-feedback. It is easy to show that the sum of the two terms adding $\mathrm{div}F_{No}$ in the right-hand side of (12) is positive when $A \in (0, A^*)$ where $0 < A^* < 1$ is the unique solution of $n_4 K_4^{n_4} - (n_4+1)K_4^{n_4} x - x^{n_4} = 0$. It is worth noting that the existence of an Helmhotz decomposition is not insured by the Helmholtz-Hodge theorem which applies for a decaying vector field that vanishes at infinity. Here, the system lies on a bounded space (the cube $[0,1]^3$) where the decomposition is not unique. It is easy to check that $\phi = k_1 A + k_2 B + k_3 C$ and $G = 0.5(k_2 C - k_3 B, k_3 A - k_1 C, k_1 B - k_2 A)^t$ satisfy $\nabla\phi = \nabla \times G$.

3.3 Steady states

Without interactions between molecules, i.e., $k_2 = k_4 = k_6 = k_7 = 0$, the oscillators have $(A, B, C) = (1, 1, 1)$ as a globally attractive steady state. The negative coupling modifies the nature of the resting state and qualitatively the new fixed points result from a balance between an attraction toward $(1, 1, 1)$ driven by the internal dynamics and an attraction toward $(0, 0, 0)$ generated by the inhibitory connection. If a static balance cannot be reached, a dynamical state induced by the negative interactions emerges with possibly the birth of oscillations.
Steady states are points in the state space where the curl-free component equals the divergence-free component of the vector field. For oscillator i, the steady state $X_0 = (A_0, B_0, C_0)$ satisfies

$$\nabla\phi_i(X_0) = \nabla \times G(X_0).$$

For the No-oscillator we obtain

$$\begin{aligned} A_0 &= (1 + r_{2,1}S_1(C_0))^{-1}, \\ B_0 &= (1 + r_{4,3}S_2(A_0))^{-1}, \\ C_0 &= (1 + r_{6,5}S_3(B_0))^{-1}, \end{aligned}$$

where $r_{p,q}$ is the ratio of rate constants k_p/k_q. The functions $f_k : x \to 1/(1 + r_k S_k(x)))$ (where $r_k = r_{2k,2k-1}$) are decreasing and thus

$$A_0 = f_1(f_3(f_2(A_0))) \tag{13}$$

has at most one solution. Since $f_1(f_3(f_2(0))) > 0$ and $f_1(f_3(f_2(x))) - x < 0$ for sufficiently large x, Eq. (13) has exactly one solution. The stability is given by the eigenvalues of the Jacobian matrix. For the NN-oscillator, using similar arguments one can show that there is exactly one steady state. However, for the PN-oscillator several steady states can coexist as shown in Fig. 2.
It is worth noting that the No-oscillator is invariant under the circulating permutation

$$\begin{aligned} k_1 &\to k_3 \to k_5 \to k_1, \\ k_2 &\to k_4 \to k_6 \to k_2, \\ K_1 &\to K_2 \to K_3 \to K_1, \\ n_1 &\to n_2 \to n_3 \to n_1. \end{aligned}$$

The symmetry is broken by the additional self-feedback loop and thus, in comparison with the No-oscillator, the possible oscillator birth or oscillator death obtained for the NN-oscillator or the PN-oscillator is induced by symmetry breaking.

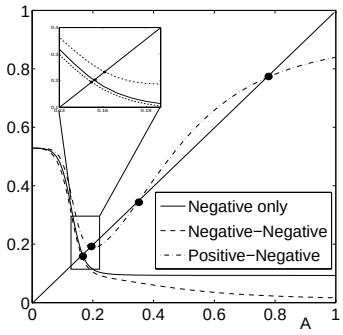

Fig. 2 Determination of the A-component of the steady states as the crossing point between the curves and the straight line $y = A$, for the different oscillators. For the negative feedback-only oscillator and the negative-plus-negative oscillator, there exists one fixed point. For the positive-plus-negative oscillator, several steady states can coexist. The inset shows a zoom on the corresponding region. Parameters are $r_{2,1} = r_{4,3} = r_{6,5} = 10$, $r_{7,1} = 100$, $K_1 = K_2 = K_4 = 0.2$, $K_3 = 0.25$ and $n_1 = n_2 = n_3 = n_4 = 3$.

3.4 The fast-slow repressilator

A qualitative understanding of the emergence of oscillations is provided by a fast-slow timescale analysis of the negative feedback oscillators. Let us consider the No-oscillator where we assume that the rate constants k_1, k_3, and k_5 are small, i.e., $k_1, k_3, k_5 \sim \epsilon$ where $\epsilon \ll 1$. If the sigmoidal interactions are sufficiently sharp, thus starting from an underthreshold initial condition (i.e., each sigmoidal function S_i is inactivated), the system evolves following the slow dynamics

$$\begin{aligned}\frac{dA}{dt} &= k_1(1-A),\\ \frac{dB}{dt} &= k_3(1-B),\\ \frac{dC}{dt} &= k_5(1-C),\end{aligned}$$

that holds as long as the concentrations of the different molecules are below their associated thresholds, i.e. $A < K_2$, $B < K_3$ and $C < K_1$. When one species reaches its threshold, the corresponding interaction is activated. Depending on the relative location of K_1, K_2, K_3 and the relative strength of the rate constants k_1, k_3 and k_5, different oscillatory patterns can be obtained. Let us assume that C reaches its threshold K_1 first. At that time, noted t_0, the concentration of molecule A follows the fast dynamic

$$\frac{dA}{dt} = -k_2 A S_1(C)$$

and quickly tends towars 0. We enter a regime where $A(t) \ll 1$ and B, C slowly tend toward 1. Let t_1 be the time at which $B(t_1) = K_3$. At that time, C tends

toward 0 following a fast dynamics whereas A enters a slow recovery process toward 1 while B continues to increase toward 1. At a time noted t_2, A reaches its threshold and subsequently B is reset to 0 whereas C starts its recovery process that will define a time t_3 such that $C(t_3) = K_1$. These different regimes repeat indefinitely giving rise to an oscillatory activity characterized by the successive resetting of variables A, B and C (fast trajectory toward 0) following by recovery processes toward 1 (see Fig. 3). It should be noted that the fast-slow repressilator presented here has a fast repressor dynamics in contrast with many synthetic oscillators where the activation is fast and repression is slow (Purcell et al. 2010).

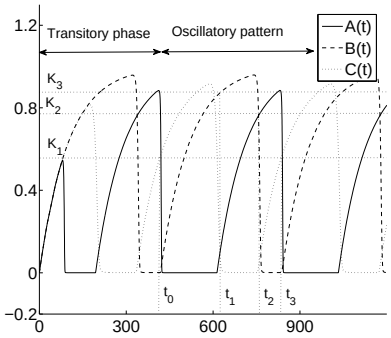

Fig. 3 Oscillatory activity of the fast-slow negative feedback-only oscillator as a function of time. Parameters are $k_1 = k_3 = k_5 = 0.01$, $k_2 = 30$, $k_4 = 10$ and $k_6 = 10$. The threshold values are $K_1 = 0.6$, $K_2 = 0.8$ and $K_3 = 0.9$. The Hill coefficients are $n_1 = n_2 = n_3 = 100$.

From the previous discussion, it is easy to show that a necessary and sufficient condition to have a periodic switch between the fast and the slow regimes is $K_i < 1$, $i = 1, 2, 3$. The analysis is valid in the limit of a sharp sigmoid, i.e., $n_i \gg 1$, and we will show in the next section that this condition prevents the occurence of stable fixed points that would lead to oscillator death.

3.5 The high cooperativity limit

The Hill functions describe the cooperative dynamics of macromolecules. Interactions of Hill type are modeled by sigmoidal functions where the slope of the curve near the median effective concentration is governed by the Hill coefficient. When the Hill coefficient is large ($n_i \gg 1$), a situation that we refer to as the high cooperativity limit (HCL), the transition around K_i is sharp and the sigmoid behaves as an Heaviside-step function generating a switch-like interaction. The functions S_i, Eq. (3), become

$$S_i(x) = \Theta(x - K_i)$$

where Θ is the Heaviside-step function and parameter K_i plays the role of a threshold. In this limiting regime, the studied oscillators belong to the class of piecewise linear differential equations and it becomes possible to derive analytical conditions for the existence of oscillations. Let us define the following critical values

$$K_1^* = \frac{k_5}{k_5+k_6}, \quad K_2^* = \frac{k_1}{k_1+k_2}, \quad K_3^* = \frac{k_3}{k_3+k_4}.$$

For the NN-oscillator, we define the two additional critical values

$$K_{4,a}^* = \frac{k_1}{k_1+k_2+k_7}, \quad K_{4,b}^* = \frac{k_1}{k_1+k_7}$$

and for the PN-oscillator, we define

$$K_4^* = \frac{k_1+k_7}{k_1+k_2+k_7}.$$

Each critical value is the ratio of the rate constants of the reaction kinetics with and without interactions. We find that the conditions for the existence of an oscillatory regime are determined by the relative location of K_i, $i = 1, 2, 3, 4$ with the associated critical values K_i^* and with unity (see appendix B.2). More precisely, for the No-oscillator, oscillations exist when

$$\begin{array}{l} K_1^* < K_1 < 1, \\ K_2^* < K_2 < 1, \\ K_3^* < K_3 < 1. \end{array} \tag{14}$$

For the NN-oscillator, the existence of oscillations is given by the following non-intersecting sets

$$\begin{array}{l} K_1^* < K_1 < 1, \\ K_2^* < K_2 < 1, \\ K_3^* < K_3 < 1, \\ K_4 > 1, \end{array} \quad \text{or} \quad \begin{array}{c} K_1^* < K_1 < 1, \\ K_{4,a}^* < K_2 < K_{4,b}^*, \\ K_3^* < K_3 < 1, \\ 0 < K_4 < K_{4,b}^*. \end{array} \tag{15}$$

For the PN-oscillator, we find

$$\begin{array}{l} K_1^* < K_1 < 1, \\ K_2^* < K_2 < 1, \\ K_3^* < K_3 < 1, \\ K_4 > K_4^*, \end{array} \quad \text{or} \quad \begin{array}{c} K_1^* < K_1 < 1, \\ K_4^* < K_2 < 1, \\ K_3^* < K_3 < 1. \end{array} \tag{16}$$

The projection of the sets (14)-(16) on the (K_2, K_4) parameter plane is shown in Fig. 4. An example of a limit cycle together with the corresponding oscillatory pattern is plotted in Fig. 5. When one of the inequalities defining the sets (14), (15) and (16) is violated, a stable fixed point appears (see appendix B.1) leading to the so-called oscillator death. When $K_4 > 1$, the additional self-feedback loop of the NN and PN-oscillator is inactive and the conditions for the existence of oscillations are identical for all oscillators, i.e.,

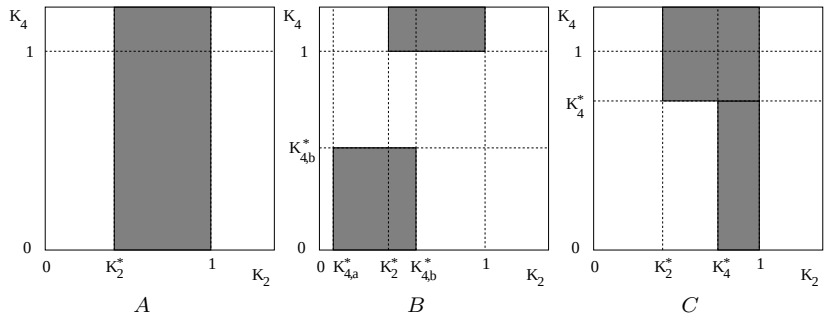

Fig. 4 Locus of existence of stable oscillations in the (K_2, K_4) parameter space (shaded grey) for (A) the negative feedback-only oscillator, (B) the negative-plus-negative oscillator and (C) the positive-plus-negative oscillator. Parameters, K_i, $i = 1, 3$, satisfied $K_i^* < K_i < 1$.

$K_i^* < K_i < 1,\ i = 1, 2, 3$. Note that in terms of the original parameters, inequalities $K_1^* < K_1 < 1$ become

$$\frac{\alpha_c}{\beta_c + \beta_{cb}} < K_c < \frac{\alpha_c}{\beta_c}.$$

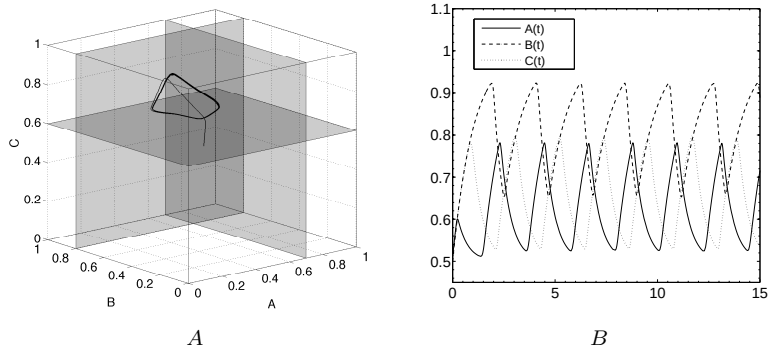

Fig. 5 Oscillations in the piecewise linear negative feedback-only oscillator. A) Limit cycle in the phase plane. The phase plane is partitioned into rectangular regions delimited by the switching planes $A = K_2$, $B = K_3$ and $C = K_1$. B) The corresponding trajectories of the three variables of the model. Parameters are $k_i = 1$, $i = 1, \ldots, 6$ and $K_1 = 0.6$, $K_2 = 0.7$,$K_3 = 0.8$. The initial condition is $(A(0), B(0), C(0)) = (0.5, 0.5, 0.5)$.

3.5.1 Remarks on oscillatory activities

The oscillatory patterns that we obtained are expected to be limit cycles, i.e. periodic trajectories. The main reason is based on the results of Mallet-Paret and Smith (1990) on smooth monotone feedback systems and its possible generalization to discontinuous systems: without stable fixed points, the trajectories of the system approach as $t \to \infty$, either a limit cycle, or a set consisting of equilibra together with homoclinic and heteroclinic orbits. In particular, chaotic solutions do not occur. Homoclinic or heteroclinic orbits do not exist in the studied systems. The proof is trivial for regular fixed points and we assume that the possible singular fixed points do not support these connecting orbits. Numerically we only observed limit cycles or fixed points.
We have here only derived sufficient conditions for the existence of oscillatory patterns. These conditions are necessary if we assume that the existence of a stable fixed point precludes the existence of stable limit cycles, i.e., bistability between a fixed point and a limit cycle is ruled out. Many negative cyclic feedback systems share this property (Tyson 1975; Hastings 1977; Hastings et al. 1977; Smith 1987; Mallet-Paret and Smith 1990; Müller et al. 2006; and other references therein) that holds for systems where oscillations occur through a supercritical Hopf bifurcation, in contrast with the subcritical Hopf bifurcation that may support bistability. Thus, we have rigorously derived only a subset of the total oscillatory domain but, numerically, we did not observe bistability. Additional complications in the analysis are generated by the nature of the flow on the switching surfaces where singular solutions may exist (Glass and Pasternack 1978a, 1978b; Snoussi and Thomas 1993; Mestl et al. 1995a,b). A rigorous treatment of these trajectories has been initiated by Filippov (1988) and further developed in the context of biological systems by Plahte and Kjoglum (2005) and by Ironi and coworkers (Ironi et al. 2011). Recently, these approaches have been revisited (Machina et al. 2013) and reformulated in the complementarity systems framework (Acary et al. 2014). Due to the particular nature of the systems studied here, there are no oscillatory trajectories with a sliding part but steady states may lie on a switching surface (see appendix B.1).

3.5.2 Links with previous work

The idealization of nonlinear functions by an Heaviside-step function to address oscillations in biological systems dates back to McKean (1970) and Hastings (1977). The resulting piecewise linear systems have been proposed as a modeling framework in biology allowing efficient simulations while being analytically tractable. Piecewise linear systems have been introduced for the study of regulatory networks (Glass and Kaufman 1973; Mest et al. 1995a; Gouzé and Sari 2002) and have been successfully applied to the qualitative simulation of genetic networks (de Jong et al. 2003). In this context, earlier results on the possible oscillatory regimes have been obtained by Glass and Pasternack (1978a) and extended in subsequent work (Snoussi 1989; Farcot

and Gouzé 2009, 2010; Lu and Edwards 2010). A common representation of the dynamics uses the so-called state transition diagram of the system (Glass and Pasternack 1978a, 1978b). In Fig. 6 we plot the state transition diagram of the No-oscillator for $k_i = 1$, $i = 1, \ldots, 6$ and $K_i = 2/3$, $i = 1, 2, 3$ showing the existence of a so-called logical cycle (where, for instance, the state 010 corresponds to the configuration $A < K_2$, $B > K_3$ and $C < K_1$). Since there is no branching point the logical cycle is a cyclic attractor of the system. To

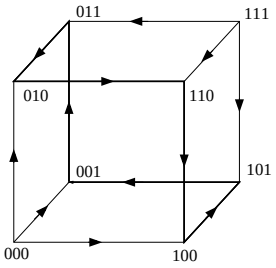

Fig. 6 State transition diagram for the negative feedback-only oscillator where $K_i^* < K_i < 1$, $i = 1, 2, 3$. The cyclic attractor is represented by heavy edges.

further compare our analysis with previous works, it is convenient to rewrite the equations in the following form:

$$\frac{dx_i}{dt} = \alpha_i(X) - \gamma_i(X)x_i, \quad i = 1, 2, \ldots, n, \tag{17}$$

where X is the boolean vector $X = (\Theta(x_1 - K_2), \Theta(x_2 - K_3), \ldots, \Theta(x_n - K_1))$, $\alpha_i(X)$ denotes the production rate and $\gamma_i(X)$ is the relative decay rate. Formulation (17) is commonly used to describe the dynamics of regulatory genetic networks (Glass and Pasternack 1978b; Mest et al. 1995a, 1995b). However, only one threshold per variable is used and thus the PN- and NN-oscillators cannot be recast in this framework. Moreover, common assumptions are: (i) that decay rates are identical and (ii) that interactions occur in the production term, in contrast with the No-oscillator studied here where the coupling alters the degradation rate

$$\gamma_i(X) = k_{2i-1} + k_{2i}X_{i-1},$$

(we define $X_0 = X_n$) and the production rate is assumed to be constant

$$\alpha_i(X) = k_{2i-1}.$$

Oscillations are therefore induced by the modulation of the decay rates and not by the time evolution of production rates. The decay rates are piecewise constant unlike the vast majority of previous work that uses constant rates and piecewise constant production terms. Moreover, another significant difference with previous work on periodic orbits (Glass and Pasternack 1978b; Farcot

and Gouzé 2009) is the architecture of the model: each variable inhibits the production of the next variable unlike systems where each variable activates the next variable except one (noted x_n) which inhibits x_1.
The cyclic attractor of the transition graph is closely related to the existence of an absorbing torus-like region for the smooth system (Buse et al. 2010) which is linked with the existence of a partition of the state space into regions where the sign of the flow remains constant. The signature of the dynamics for both the discontinuous and smooth systems remains the same (Buse et al. 2009): $(110) \to (100) \to (101) \to (001) \to (011) \to (010)$ which is remiscent to the functioning of the ring oscillator in electronics (an odd number of not gate in series forming a chain).
Finally, a closely related study in term of methodology has been performed by Matsuoka (1985) in the field of neurosciences. Sufficient conditions for oscillations in neural networks are derived from stability analysis. Similarly to our approach, the author uses a step function to idealize the nonlinearities, considers inhibitory connections and focuses on circular architectures. Analytical expressions on network structure are obtained for a neural system to generate and sustained oscillations (including chaotic solutions).

3.5.3 Probability of oscillations

A Monte Carlo approach has been used by Tsai and coworkers (Tsai et al. 2008) to explore in the parameter space the domain of existence of stable limit cycles. They generated random parameter sets for the three different oscillators and determined by numerical integration of the equations whether oscillatory regimes are observed. One of the goals of this paper is to provide an analytical understanding of the previous results numerically obtained (see Fig. 4 in Tsai et al. 2008). On the other hand, the probability of oscillations gives a quantitative assessment of the robustness of oscillations.
In the limit $n_i \to \infty$ we have obtained in the previous section the domain of existence of oscillatory activities. In this section, we will derive analytically the probability of oscillations for the different oscillator models.
Negative feedback-only oscillator. Let P_{No} be the probability of the No-oscillator oscillating. We have

$$P_{No} = \prod_{i=1,2,3} P(K_i^* < K_i < 1),$$

or equivalently

$$P_{No} = \prod_{i=1,2,3} \left(1 - P(K_i > 1) - P(K_i < K_i^*)\right).$$

To compare with the numerical results obtained in (Tsai et al. 2008) we use the same assumptions on the parameters of the model: the thresholds, K_i, $i = 1, 2, 3$, are random variables that follow continuous uniform distributions on $[0, \bar{K_i}]$ and we note $K_i \sim U(0, \bar{K_i})$ where $(\bar{K_i})$ are positive constants that we

assume greater than 1 for simplicity. We also assume that the rate constants k_j, $j = 1, \ldots, 6$ satisfy $k_i \sim U(0, \bar{k}_i)$.
We have

$$P(K_i > 1) = 1 - \frac{1}{\bar{K}_i}. \tag{18}$$

Using $K_1^* = k_5/(k_5 + k_6)$, we obtain

$$P(K_1 < K_1^*) = \frac{1}{\bar{K}_1 \bar{k}_5 \bar{k}_6} \int_0^{\bar{k}_6} \int_0^{\bar{k}_5} \frac{x}{x+y} dxdy. \tag{19}$$

We define

$$F(x) = \frac{\ln(1+x)}{x} \tag{20}$$

and we calculate

$$P(K_1 < K_1^*) = \frac{1}{2\bar{K}_1} \left(F\left(\frac{\bar{k}_6}{\bar{k}_5}\right) - F\left(\frac{\bar{k}_5}{\bar{k}_6}\right) + 1 \right) \tag{21}$$

and similar equations hold for the expressions of $P(K_2 < K_2^*)$ and $P(K_3 < K_3^*)$.
Let (H) be the following assumption: the thresholds (K_i), $i = 1, 2, 3$, the self-rate constants (k_{2i-1}) and the coupling rate constants (k_{2i}) have identical and independent uniform distributions (as in Tsai et al. 2008). We note

$$(H) \begin{cases} K_i \sim U(0, K), \\ k_{2i-1} \sim U(0, k) \\ k_{2i} \sim U(0, k_c) \end{cases} \tag{22}$$

where $K \geq 1$, $k > 0$, and $k_c > 0$ where the subscript "c" stands for "coupling". The probability of oscillations for the No-oscillator is given by

$$P_{No} = \frac{1}{8K^3} \left(1 + F(r_c) - F\left(\frac{1}{r_c}\right) \right)^3 \tag{23}$$

where r_c is the ratio of the maximal value of the self-rate constant over the maximal value of the coupling rate constant, i.e. $r_c = k/k_c$. Probability (23) is maximum when $r_c \to 0$, and, for small r_c values, we derive the following asymptotic expansion:

$$P_{No} = \frac{1}{K^3} \left(1 - \frac{3}{4} r_c + \frac{3}{2} r_c \ln r_c \right) + r_c \epsilon(r_c), \tag{24}$$

where $\epsilon(r_c) \to 0$ as $r_c \to 0$. For parameters used in (Tsai et al. 2008) (see appendix C) we find $P_{No} = 0.01446$. Approximation (24) gives $P_{No} = 0.01443$ and if we keep only the first term of the expansion we find $P_{No} = 0.01562$.

In (Tsai et al. 2008) the value of k_5 has been fixed to 1 and therefore $K_1^* = (1+k_6)^{-1}$. Expression (19) becomes

$$P(K_1 < K_1^*) = \frac{1}{\bar{K}_1 \bar{k}_6} \int_0^{\bar{k}_6} \frac{dy}{1+y}$$

which gives

$$P(K_1 < K_1^*) = \frac{1}{\bar{K}_1} F(\bar{k}_6)$$

and we find $P(K_1 < K_1^*) = 1.72\ 10^{-3}$ (instead of $P(K_1 < K_1^*) = 6.39\ 10^{-3}$ when $k_5 \sim U(0,k)$) that yields $P_{No} = 0.0147$. It can be seen that the probability is poorly modified by the distribution of the random variable k_5. Indeed, parameter k_5 acts on P_{No} through the critical parameter K_1^* but does not affect significantly its distribution. As a consequence, the influence of the k_5 distribution on P_{No} is weak.

Negative-plus-negative oscillator. For the NN-oscillator, we assume that the parameters of the self-feedback loop satisfy $k_7 \sim U(0,\bar{k}_7)$ and $K_4 \sim U(0,\bar{K}_4)$. From (15) the probability of oscillations for the NN-oscillator is given by

$$\begin{aligned} P_{NN} = {} & P_{No} P(K_4 > 1) \\ & + P(K_1^* < K_1 < 1) P(K_{4,a}^* < K_2 < K_{4,b}^*) P(K_3^* < K_3 < 1) P(K_4 < K_{4,b}^*). \end{aligned}$$

Both probabilities $P(K_1^* < K_1 < 1)$ and $P(K_3^* < K_3 < 1)$ have been previously calculated analytically (see 18 and 21). We have $P(K_4 > 1) = 1 - 1/K_4$ and both probabilities, $P(K_4 < K_{4,b}^*)$ and $P(K_2 < K_{4,b}^*)$, are given by (21) substituting $\bar{k}_7/\bar{k}_1$ to $\bar{k}_6/\bar{k}_5$ and using $\bar{K}_4$ and $\bar{K}_2$, respectively, instead of $\bar{K}_1$. To complete the analytical expression of P_{NN}, it remains to calculate $P(K_2 < K_{4,a}^*)$. We get

$$P(K_2 < K_{4,a}^*) = \frac{1}{\bar{K}_2 \bar{k}_1 \bar{k}_2 \bar{k}_7} \int_0^{\bar{k}_1} \int_0^{\bar{k}_2} \int_0^{\bar{k}_7} \frac{x}{x+y+z} dx dy dz \tag{25}$$

which has an analytical expression given in appendix B.3 (Eq. (33)).
Assuming that (H) holds, we obtain

$$\begin{aligned} P_{NN} = {} & P_{No} \left(1 - \frac{1}{K}\right) \\ & + \frac{1}{16K^4} \left(1 - F\left(\frac{1}{r_c}\right) + F(r_c)\right)^2 \left(1 + F\left(\frac{1}{r_s}\right) - F(r_s)\right) \\ & \times \left(1 + F\left(\frac{1}{r_s}\right) - F(r_s) - 2K I_{NN}\right) \end{aligned}$$

where I_{NN} is the integral in the right-hand side of (25) and $r_s = k/\bar{k}_7$ measures the strength of the self-feedback loop. Taking the limit $r_c \to 0$, we have $I_{NN} \to 0$, which yields

$$P_{NN} = \frac{1}{K^3}\left(1 - \frac{1}{K}\right) + \frac{1}{4K^4}\left(1 + F\left(\frac{1}{r_s}\right) - F(r_s)\right)^2 + \epsilon(r_c). \qquad (26)$$

To compare with the No-oscillator, we calculate the zero-order expansion of the ratio of probabilities

$$\frac{P_{NN}}{P_{No}} = 1 - \frac{1}{K} + \frac{1}{4K}\left(1 + F\left(\frac{1}{r_s}\right) - F(r_s)\right)^2$$

for small r_c values. The ratio is maximum when $r_s \to \infty$ and we have $P_{NN}/P_{No} \to 1$, corresponding to the case where $k_7 \to 0$, i.e., the self-feedback is inactivated and the two oscillators coincide. The minimum is reached for $r_s \to 0$ (strong self-feedback) and we have $P_{NN}/P_{No} \to 1 - 1/K$. Expression (26) has been derived assuming $r_c/r_s \to 0$ and therefore we only capture the limiting regime $r_c \to 0$, $r_s \to 0$, and $r_c/r_s \to 0$, i.e., the coupling strength remains greater (of at least one order) than the self-feedback strength.
For a strong self-feedback and a strong coupling, both of the same order, we consider $r_c = r_s = r \ll 1$, and, from the complete expression of P_{NN}, we calculate

$$P_{NN} = \frac{1}{K^3}\left(1 - \frac{1}{K}\right) + \epsilon(r) \qquad (27)$$

which coincides with the asymptotic development (26) when $r_s \to 0$.
For parameters used in (Tsai et al. 2008) (see appendix (C)), we find $P_{NN} = 0.0109$ using the exact analytical expression. Asymptotic expansion (26) gives $P_{NN} = 0.0118$. In the so-called "strong positive feedback" case, i.e., $r_c = r_s = 0.01$, we find $P_{NN} = 0.0108$ and approximation (27) gives 0.0117.
Positive-plus-negative oscillator. As for the NN-oscillator, we take $k_7 \sim U(0, \bar{k}_7)$ and $K_4 \sim U(0, \bar{K}_4)$. From (16) the probability of oscillations for the PN-oscillator is given by

$$\begin{aligned} P_{PN} = {} & P_{No}P(K_4 > K_4^*) \\ & + P(K_1^* < K_1 < 1)P(K_4^* < K_2 < 1)P(K_3^* < K_3 < 1)P(K_4 < K_4^*). \end{aligned}$$

All the probabilities occuring in the expression of P_{PN} have been calculated analytically hereinabove except $P(K_4 < K_4^*)$ and $P(K_2 < K_4^*)$. We have

$$P(K_4 < K_4^*) = \frac{1}{\bar{K}_4\bar{k}_1\bar{k}_2\bar{k}_7}\int_0^{\bar{k}_1}\int_0^{\bar{k}_2}\int_0^{\bar{k}_7}\frac{x+z}{x+y+z}dxdydz$$

which can be rewritten as

$$P(K_4 < K_4^*) = \frac{1}{\bar{K}_4} - I_{PN}$$

where

$$I_{PN} = \frac{1}{\bar{K}_4\bar{k}_1\bar{k}_2\bar{k}_7}\int_0^{\bar{k}_1}\int_0^{\bar{k}_2}\int_0^{\bar{k}_7}\frac{y}{x+y+z}dxdydz$$

has been previously calculated analytically (from Eq. 25, switching k_2 and k_1). A similar expression holds for $P(K_2 < K_4^*)$.
Assuming that (H) holds, we calculate

$$P_{PN} = P_{No}\left(1-\frac{1}{K}+I_{PN}\right)+\frac{1}{4K^2}\left(1+F(r_c)-F\left(\frac{1}{r_c}\right)\right)^2 I_{PN}\left(\frac{1}{K}-I_{PN}\right).$$

Taking the limit $r_c \to 0$ we get $I_{PN} \to 1/K$ and we obtain

$$P_{PN} = \frac{1}{K^3}+\epsilon(r_c) \tag{28}$$

that yields $P_{NP}/P_{No} \to 1$. The limit does not depend on r_s unlike the NN-oscillator. For a strong negative coupling and a strong self-feedback, we note $r = r_c = r_s \to 0$. We find $I_{PN} \to 1/(2K)$ and we calculate

$$P_{PN} = \frac{1}{K^3}\left(1-\frac{1}{4K}\right)+\epsilon(r) \tag{29}$$

that is lower than the limit (28) obtained as $r_c \to 0$ and r_s fixed.
For $K = 4$, $r_c = 0.01$ and $r_s = 0.1$, we find $P_{PN} = 0.01438$ using the exact analytical expression and we find $P_{PN} = 0.01562$ using (28). When $r_c = r_s = 0.01$, i.e. strong coupling and strong self-feedback, we have $P_{PN} = 0.01356$ and approximation (29) gives 0.01367.
Probabilities of oscillations as a function of the coupling ratio r_c are plotted Fig. 7 for the three oscillators. Different values for the self-feedback ratio are used. Probability of oscillations for the different models decreases with r_c suggesting that strong negative coupling facilitate oscillations. The addition of a negative self-feedback reduces the chance to oscillate whereas a moderate positive self-feedback does not modify significantly the probability of oscillations as shown in Fig. 8. The plot (Fig. 8) also indicates that, for the No-oscillator and NN-oscillator, the high-cooperativity regime gives an upper approximation of the probability of oscillations comparing to the smooth case whereas a lower approximation is obtained for the PN-oscillator. The effect of a negative or a positive self-feedback loop is illustrated in detail Fig. 9 where the probability is plotted as a function of r_s for different r_c values. It is shown that the probability of oscillations is an increasing function of r_s and crucially depends on the coupling ratio r_c. As the self-feedback ratio r_s increases a sigmoid-type transition occurs from a low-probability level to a higher probability level. The transitions for the PN- and NN-oscillators are compared in Fig. 10. The high-probability level is reached when $r_s \to +\infty$ (weak self-feedback). This level can be maintained for a large range of r_s values when the self-feedback loop is positive. However, when $r_c \gg 1$ the difference induced by the nature of the

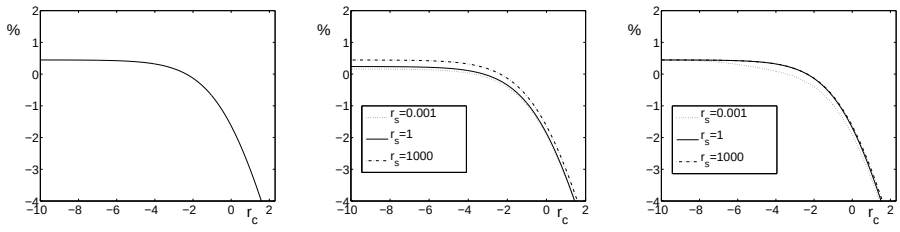

Fig. 7 Log-log plot of the percentage of parameter sets that yield stable oscillations as a function of the coupling ratio, $r_c = k/k_c$, for the negative feedback-only oscillator (left panel), negative-plus-negative oscillator (middle panel) and positive-plus-negative oscillator (right panel). For the two last oscillators, the percentage is computed for different values of the self-feedback ratio $r_s = k/\bar{k}_7$. To avoid heavy notation the axes are labeled as 'u' instead of '$log(u)$' where $u = r_c$ for the x-axis and u is the percentage of parameter sets for the y-axis.

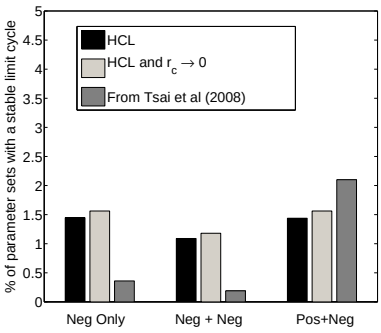

Fig. 8 Percentage of parameter sets that yield stable oscillations. Each group is for an oscillator: the negative feedback-only oscillator (left group), the negative-plus-negative oscillator (middle group) and the positive-plus-negative oscillator (right group). The black bar is for the high cooperativity limit (HCL) with a coupling ratio $r_c = 0.01$ and a self-feedback ratio $r_s = 0.1$. The middle bar represents the maximum probability obtained as the coupling ratio r_c tends towards 0 (strong coupling). The right bar represents the result of the numerical investigations in the smooth case.

self-feedback connection vanishes and the probability of oscillations becomes negligible.

The strong coupling regime ($r_c \ll 1$) is related to the fast-slow repressilator previously discussed and is revealed to be the configuration that maximizes the chance to function in an oscillatory regime. Moreover, when the strength of the self-feedback is also strong, we found, for $r_s = r_c \ll 1$,

$$P_{NN} = \frac{1}{K^3}\left(1 - \frac{1}{K}\right),$$
$$P_{PN} = \frac{1}{K^3}\left(1 - \frac{1}{4K}\right)$$

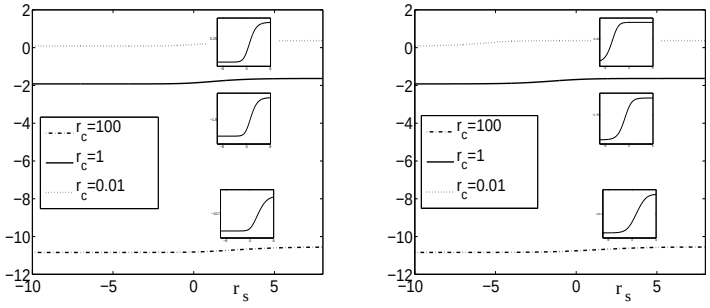

Fig. 9 Log-log plot of the percentage of parameter sets that yield stable oscillations as a function of the self-feedback ratio, $r_s = k/\bar{k}_7$, for the negative-plus-negative oscillator (left panel) and positive-plus-negative oscillator (right panel). The percentage is computed for different values of the coupling ratio: $r_c = 100$, $r_c = 1$ and $r_c = 0.01$. The insets are rescaling of the Y-axis of the corresponding curve (see also Fig. 10). Same labeling convention as in Fig. 7.

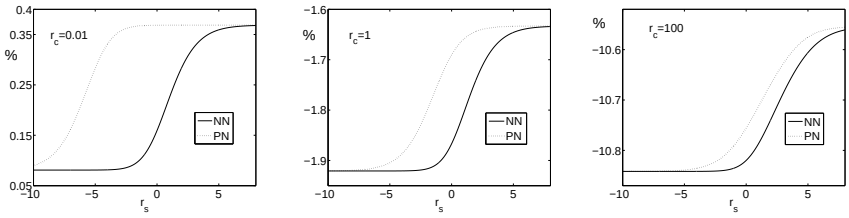

Fig. 10 Log-log plot of the percentage of parameter sets that yield stable oscillations as a function of the self-feedback ratio for different values of the coupling ratio. The negative-plus-negative oscillator is compared with the positive-plus-negative oscillator for different values of the coupling ratio: $r_c = 0.01$ (left), $r_c = 1$ (middle) and $r_c = 100$ (right). Same labeling convention as in Fig. 7.

which has $P_{NN} = 3^3/4^4 \approx 0.1055$ and $P_{PN} = 3/4$ as a maximum when $K = 4/3$ and $K = 1$, respectively.

3.5.4 Helmholtz decomposition of the piecewise linear oscillators

In the HCL, the functions (6) and (7) can be simplified as follows:

$$S_i^{[1]}(x) = (x - K_i)\Theta(x - K_i),$$
$$S_i^{[2]}(x) = \frac{1}{2}(x - K_i)^2\Theta(x - K_i)$$

and the scalar potential (9) can be rewritten as quadratic function combined with step functions. It is straightforward to show that the potential functions of the oscillators admit a global minimim. Oscillations are therefore generated by

a balance between an attracting fixed point where the gradient part vanishes and a rotating part derived from the potential vector

$$G(A,B,C) = \begin{pmatrix} k_6 C(B-K_3)\Theta(B-K_3) \\ k_2 A(C-K_1)\Theta(C-K_1) \\ k_4 B(A-K_2)\Theta(A-K_2) \end{pmatrix}.$$

For the No-oscillator and for parameters satisfying (14), the minimum of the potential function is given by

$$(A_m, B_m, C_m) = \left(\frac{k_1 + k_4 K_2}{k_1 + k_4}, \frac{k_3 + K_3 k_6}{k_3 + k_6}, \frac{k_5 + K_1 k_2}{k_5 + k_2} \right).$$

If $K_i > 1$, the corresponding minimum is 1. Therefore, the necessary condition for the existence of a limit cycle $K_i < 1$ can be reformulated as: the minimum point of the potential energy has to be greater than the median effective concentration (component by component).
For the NN-oscillator, the additional term in the potential energy can be rewritten as

$$\tilde{\phi}_{NN}(A) = \frac{k_7}{2}(A^2 - K_4^2)\Theta(A - K_4).$$

The minimum point remains unchanged if $A_m < K_4$ and a sufficient condition is $K_4 > 1$ corresponding to the upper zone of existence of limit cycles (see Fig. 4B). In this case, the minimum point A_m is lower than the median effective concentration K_4 but greater than K_2. For the other set of parameter values yielding oscillations (bottom left part of Fig. 4B), the minimum is given by

$$A_m = \frac{k_1 + k_4 K_2}{k_1 + k_4 + k_7},$$

and B_m, C_m remain unchanged. Thus $A_m > K_2$ is equivalent to the necessary condition $K_2 < K_{4,b}$ previously derived (when $K_4 < 1$).
For the PN-oscillator, we have

$$\tilde{\phi}_{PN}(A) = \frac{k_7}{2}(A - K_4)(A + K_4 - 2)\Theta(A - K_4).$$

The minimum stays unchanged if $A_m < K_4$, otherwise the minimum becomes

$$A_m = \frac{k_1 + k_7 + k_4 K_2}{k_1 + k_4 + k_7}.$$

In both cases $A_m > K_2$ reads $K_2 < 1$.

3.6 The smooth case: numerical analysis of oscillatory regimes

In this section, we will investigate numerically the smooth sigmoidal case and we will determine the domain of existence of stable oscillations in the parameter space together with the size and location of the limit cycles.

3.6.1 Domain of oscillations

We redid the numerical experiments of Tsai and coworkers (Tsai et al. 2008): for the different oscillators, we generated random parameter sets (see appendix C) until we had obtained 500 that gave stable oscillations. The distributions of parameters $(K_i)_{i=1,\dots,4}$ that give oscillations are represented with histograms shown in Fig. 11A-C for the three different oscillators. Figures 11D, E shows the distributions in the (K_2, K_4) plane for the NN- and PN-oscillator and Fig. 11F-H shows the distributions of the Hill coefficients. Figure 11 indicates that

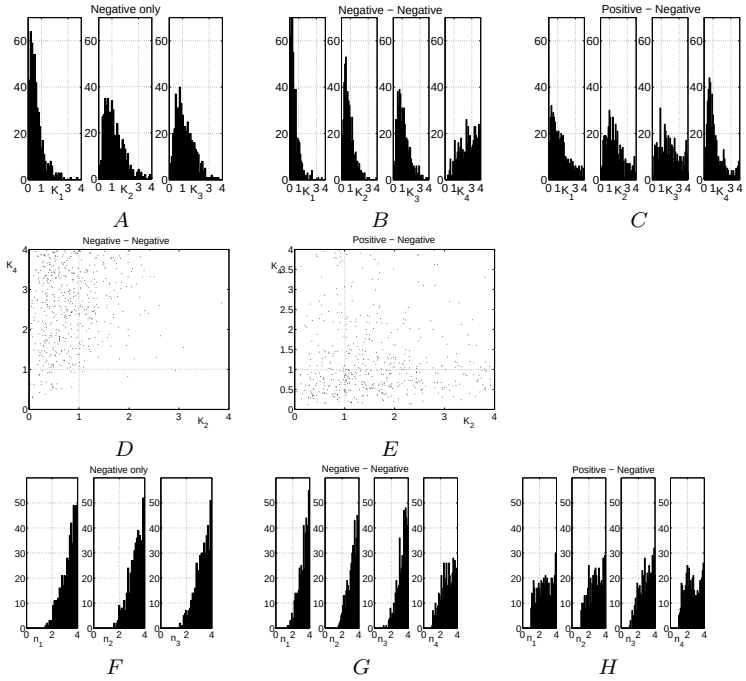

Fig. 11 Distributions of parameters leading to oscillations for the different oscillator models. A Histograms of K_1, K_2 K_3 for the negative feedback-only oscillator and of K_1, K_2, K_3, K_4 for B the negative-plus-negative oscillator and C the positive-plus-negative oscillator. The histograms are computed for 500 parameter sets that gave oscillations for each oscillator. The projections of the distributions in the (K_2, K_4) parameter space are shown panel D and E for the negative-plus-negative oscillator and for the positive-plus-negative oscillator, respectively. Histograms of the distributions of the Hill coefficients, $(n_i)_{i=1,\dots,4}$, are shown panels F-H (models as for A-C respectively).

there is no significant difference in the distribution of parameters between the No-oscillator and the NN-oscillator. The nonsymmetric distribution of parameters $(K_i)_{i=1,2,3}$ observed for the No-oscillator is only due to the fact that k_5 has been fixed to 1. The histograms of the median effective concentrations are peaked near a value slightly less than 1 (reminiscent to the condition for

oscillations $K_i < 1$ obtained for the step-like coupling) whereas the Hill coefficients are mainly located at large values. Therefore, a high cooperativity facilitates oscillatory activities and explained the upper approximation of the probability of oscillations obtained when $n_i \gg 1$. The existence of a positive self-feedback loop makes more uniform the distributions of parameters indicating weak constraints on parameters for limit cycle existence. Parameter K_4 of the NN-oscillator has to be large (greater than 1) suggesting that the additional negative self-feedback loop is preferentially inactivated during oscillations whereas the positive loop plays an enhancing role in oscillatory regimes (K_4-histogram peaks for a value less than 1). For the PN-oscillator, a local peak of the n_4-histogram occurs close to $n_4 = 2$ suggesting that moderate n_4 values also facilitates oscillations and therefore explains why the probability of oscillations in the HCL gives a lower approximation of the corresponding probability for n_4 finite (see Fig.8).

3.6.2 Location and size of limit cycles

In order to assess the location and the size of the limit cycles, we compute for the three different oscillators and for each variable of the model: (i) the mean value $\bar{X} = 1/T \int_0^T X(t)dt$ for $X = A(t)$, $B(t)$ or $C(t)$ and (ii) the peak amplitude $|X| = \max X(t) - \min X(t)$ where $(A(t), B(t), C(t))$ is the limit cycle solution and T the period of the oscillations. Results are shown in Fig. 12. It can be seen that the PN-oscillator supports a larger variability in the

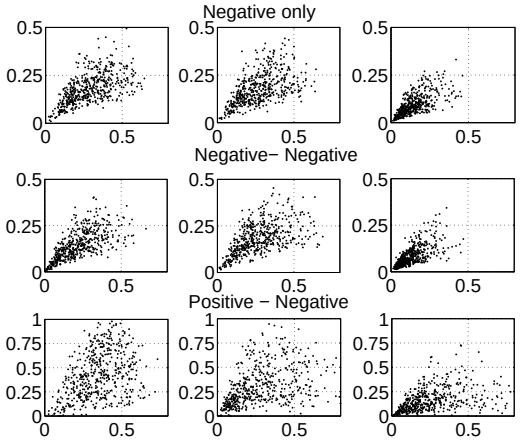

Fig. 12 Plots of the peak amplitude as a function of the mean location of the limit cycles for the three different oscillators. The first row is for the oscillator without self feedback, the second one is for the negative-plus-negative oscillator and the third one is for the positive-plus-negative oscillator. The left column is for the A variable, the middle one is for B and the right one is for C. A different scale of the vertical axis has been used for the positive-plus-negative oscillator.

amplitude and location of its limit cycle whereas the No-oscillator and NN-oscillator exhibit similar properties. This is also illustrated in Fig. 13 where some limit cycles are plotted in the phase space. A larger filling is obtained for the PN-oscillator. Results suggest that the addition of a positive self-feedback loop produces a higher variability and thus enhances the tunability of the system.

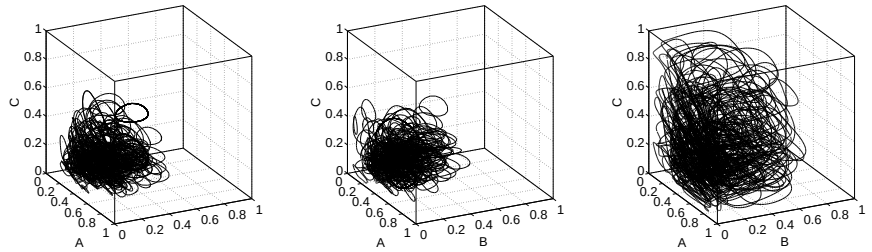

Fig. 13 Plots of the limit cycles in the state space (250 limit cycles have been plotted) for the negative feedback-only oscillator (left), the negative-plus-negative oscillator (middle) and positive-plus-negative oscillator (right).

3.7 A generalized repressilator-type model

The core pathway motif that underpins sustained oscillations may involve more than three components. A generalization of the cyclic biochemical circuit to an arbitrary number N of components sequenced in series, schematically represented by $x_1 \dashv x_2 \dashv \ldots \dashv x_N \dashv x_1$, is given by:

$$\frac{dx_i}{dt} = k_{2i-1}(1 - x_i) - k_{2i}x_i S_i(x_{i-1}), \quad \text{for} \quad i = 1, \ldots, N,$$

where x_i is the dimensionless concentration of the chemical species i and we define $x_0 = x_N$ making the system of equations into a cycle. Parameters k_{2i-1} and k_{2i} are kinetic constants, K_i are the dissociation constants, and S_i are the sigmoidal functions given by (3). Here, we restrict our attention to a network without self-feedback loop. Each species is repressed (inhibited) by the species immediately preceding in the loop. The network architecture is based on the successive inhibition of the chemical species and follows the design principles of the repressilator. A similar but different generalized model of repressilator-type has been proposed and studied in (Müller et al. 2006).
For a switch-like coupling obtained in the limit of large Hill coefficients, the equations become

$$\frac{dx_i}{dt} = k_{2i-1}(1 - x_i) - k_{2i}x_i \Theta(x_{i-1} - K_i), \quad \text{for} \quad i = 1, \ldots, N.$$

Shifting the origin to the point of intersection of all thresholds, the system could be rewritten as

$$\frac{dx_i}{dt} = a_i(x_i) - b_i(x_i)\mathrm{sgn}(x_{i-1}), \quad \text{for} \quad i = 1, \ldots, N,$$

where $a_i(x) = k_{2i-1} - (k_{2i-1} + k_{2i}/2)(x + K_{i+1})$, $b_i(x) = k_{2i}/2(x + K_{i+1})$, sgn is the sign function, and we set $K_{N+1} = K_1$.
An analysis (not shown) similar to the one performed for the three-component oscillator gives

– if N is odd, oscillatory regimes are obtained for

$$K_i^* < K_i < 1, \quad i = 2, \ldots, N \quad \text{where}$$
$$K_i^* = \frac{k_{2i-3}}{k_{2i-3} + k_{2i-2}}, \tag{30}$$

  where $k_0 = k_{2N}$ and $k_{-1} = k_{2N-1}$.
– if N is even, the network admits at least one stable fixed point. In particular, for parameters belonging to the domain of periodic behavior obtained for the negative feedback system, i.e., (30), it can be shown that the network exhibits bistability between the two stable steady states

$$(1, K_3^*, 1, \ldots, K_{N-1}^*, 1, K_1^*) \quad \text{and} \quad (K_2^*, 1, K_4^*, \ldots, 1, K_N^*, 1)$$

  This situation is similar to the one encountered for the two-component system where it is easy to see that $(1, K_1^*)$ and $(K_2^*, 1)$ are two stable fixed points that coexist if and only if $K_1^* < K_1 < 1$ and $K_2^* < K_2 < 1$.

The qualitative difference in the dynamics of cyclic feedback systems with an odd or an even number of elements in the cycle has already been pointed out by Fraser and Tiwari (1974), studied by Smith (1987), and subsequently in (Mallet-Paret and Smith 1990; Müller et al. 2006). It has been shown that this difference mainly manifests for strong nonlinearities whereas for weak nonlinearities the number of molecules involved in the loop does not play a crucial role in the dynamics. An even number of negative interactions canceled each other and the network essentially acts as a positive feedback system. The fundamental difference between both networks is related to the competitive nature of negative feedback systems whereas positive feedback systems are of cooperative and irreducible nature in the sense of Hirsch (1982, 1985). For cooperative systems, almost all trajectories tend to a steady state that always exists for N even.
For an odd number of nodes and for uniformly distributed parameters, i.e., $K_i \sim U(0, \bar{K}_i)$, $i = 1, \ldots, N$ and $k_i \sim U(0, \bar{k}_i)$, $i = 1, \ldots, 2N$, the probability of oscillations is given by

$$P_{No} = \prod_1^N \frac{1}{2\bar{K}_i} \left(1 - F\left(\frac{\bar{k}_{2i-2}}{\bar{k}_{2i-3}}\right) + F\left(\frac{\bar{k}_{2i-3}}{\bar{k}_{2i-2}}\right)\right)$$

where we define $\bar{k}_0 = \bar{k}_{2N}$ and $\bar{k}_{-1} = \bar{k}_{2N-1}$. The function $F(x)$ is given by (20). For dissociation constants with identical maximal values, $\bar{K}_i = K$, and for identical ratios of maximum rate constants, $r_c = \bar{k}_{2i-1}/\bar{k}_{2i}$, we obtain

$$P_{No} = \frac{1}{2^N K^N} \left(1 + F(r_c) - F\left(\frac{1}{r_c}\right)\right)^N. \tag{31}$$

Probability (31) is represented in Fig. 14A as a function of r_c for different N values. In the limit of a strong coupling (or weak internal dynamics), i.e.

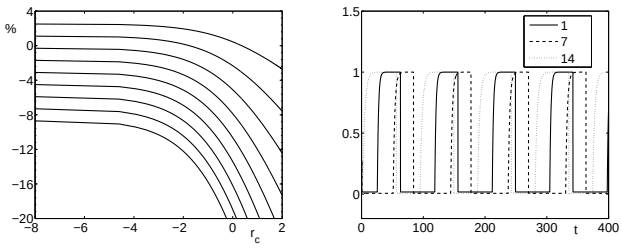

A *B*

Fig. 14 A. Log-log plot of the percentage of parameters leading to oscillation as a function of the coupling ratio r_c for different lengths of the negative feedback oscillator. Probabilities obtained for odd N values from $N = 3$ (upper) to $N = 19$ (lower) are depicted. We used $K = 2$. Same labeling convention as in Fig. 7. B. Oscillations in a circular negative feedback system of $N = 19$ nodes. Parameters K_i, k_{2i} and k_{2i} are uniformly distributed on $(0, 1)$, $(0, 100)$ and $(0, 1)$, respectively ($r_c = 0.01$). Activity of elements $i = 1, 7, 14$ is represented (starting from a random initial condition in $[0, 1]^N$).

$r_c \ll 1$, we obtain the following asymptotic expansion of the probability of oscillations

$$P_{No} = \frac{1}{K^N} + \frac{N r_c}{2K^N} \ln(r_c) + r_c O(1). \tag{32}$$

Some typical trajectories of network elements are shown Fig.14B for a network of $N = 19$ nodes with a weak r_c value. The activity is characterized by sequential successions of active and inactive states. Probability (31) vanishes as N becomes large except for $K = 1$ and for sufficiently small r_c values. More precisely, a non-zero probability is reached if and only if $r_c N \ll 1$, i.e. r_c has to be sufficiently small with respect to N, or equivalently a necessary and sufficient condition is $N r_c^\beta$ bounded $\forall \beta < 1$.

4 Discussion

In the present work, based on a mathematical and numerical analysis of repressilator-type oscillators, we corroborated and characterized some observations already made or proved in various biological systems. (i) Oscillations

are promoted by negative feedbacks. (ii) Strong nonlinearities facilitate oscillations: the more switch-like are the interactions, the easier it is to generate oscillations. (iii) A qualitative difference in the dynamics of monotone cyclic feedback systems occurs between an even or an odd number of components in the cycle. (iv) A strong inhibitory coupling induces a fast-slow dynamics that maximizes the probability of oscillations. In this regime, the dynamics is characterized by sequential switches from active to inactive states and vice-versa. (v) Small molecular circuits are suitable candidates to design robust biological oscillators. Moreover, as the length N of the feedback loop increases, the coupling strength $1/r_c$ has to increase in order to maintain the product Nr_c sufficiently small. Therefore, the claim "the longer the loop, the easier it is to produce oscillations" (see, for instance Ferrell et al. 2011) is not fully corroborated by our study. However we used here a restrictive framework where interactions are step-like, which seems unlikely in many biological systems. It is suspected that a longer cycle allows to weaken the stiffness of nonlinearities (Smith 1987) and a balance between "moderate" Hill coefficients, sufficiently long feedback loop and strong inhibitory coupling should be reached to maximize the chance of oscillations.

Some features of the smooth oscillators are preserved by the step-like coupling. In particular, an additional negative feedback severely reduces the possibility of oscillations of cyclic negative feedback systems. However, some discrepancies are observed: comparing to the smooth case, a step-like coupling promotes oscillations except for the PN-oscillator where oscillatory regimes appear at moderate values of the Hill coefficients and therefore an additional positive feedback does not enhance oscillations in the sharp-coupling case, unlike the smooth case. Moreover, we have shown that the PN-oscillator allows a large variability in the amplitude of oscillations. Surprisingly, it has been reported in the smooth case (Tsai et al. 2008) that a positive feedback provides a tunable frequency and constant amplitude. This counterintuitive result is probably due to a distinct role played by the parameters of the system: the amplitude and the frequency of oscillations can be tuned separately varying different parameters.

Adding a negative self-feedback loop in a negative cyclic feedback oscillator does not present any new advantages whereas a moderate positive self-feedback weakens the constraints on parameters in the oscillatory regime and improves the versatility of the system. Tunability induced by positive loops has already been observed in molecular systems (Tsai et al. 2008; López-Caamal et al. 2013) and is essential in cases where cellular processes require a tight regulation. The additional self-feedback loop affects the structure of the flow of the three components system and modifies the Helmholtz decomposition of the oscillators. The divergence-free part of the decomposition, analog to a circulating density responsible for a vortex-like behavior, remains unchanged but the gradient part that minimizes the corresponding potential energy is affected. A positive self-feedback loop increases the divergence of the system and facilitates oscillations whereas a negative self-feedback loop tends to stabilize the system on a steady state precluding oscillations.

There are various ways of taking into account the fluctuations inherent in real systems. Two different frameworks have been used to address the issue of randomness and limit cycles: random environments (Lin and Kahn 1977) and uncertain environnements (Falkenburg 1979). Here we considered random parameters but the presence of a stochastic term in the nonlinear differential system may induce different properties. A stochastic switching between two stable states has been observed in three-node genetic regulatory networks (Li et al. 2012). It has been shown that the unstable periodic solution of repressilator-type networks with an even number of nodes can be stabilized with random walk noise (Strelkowa and Barahona 2010). This suggests that oscillations are more widespread than expected by the study of the deterministic system and the probability of oscillations may be enhanced by a Brownian noise.
Determining the conditions for robust oscillations has attracted a renewal of interest with the emergence of synthetic biology (Elowitz and Leibler 2000; Stricker et al. 2008; Gardner et al. 2000). It has become possible to construct in the laboratory a biological system according to "design specifications" derived from analytical and/or computational approaches. Networks of interacting species (mainly gene networks) are shaped in order to perform a given function, and due to its fundamental role in cellular processes, oscillations have attracted much attention. The calculation of the probability of oscillations when fluctuating parameters are considered is of particular interest in this engineering-based approach. Despite the fact that parameters of a real biological system are probably not uniformly distributed with independent distribution, our approach suggests a way to tackle this issue and, as far as we know, we obtained for the first time a close form expression for the probability of oscillations in a nonlinear dynamical system. Without specific knowledge on the distribution of parameters, the uniform probability distribution is a natural choice that requires less a priori information on the underlying processes. However, it has been shown that kinetic rate parameters are more likely to follow Benford's law (Grandison and Morris 2008) and the study of the probability of oscillations for log-uniform distributions is desirable.

A Appendix: Jacobian matrix of the smooth system

For the negative feedback-only oscillator, the Jacobian matrix is given by

$$J_{No}=\begin{pmatrix} -k_1-k_2S_1(C) & 0 & -\frac{k_2n_1K_1^{n_1}C^{n_1-1}}{(K_1^{n_1}+C^{n_1})^2}A \\ -\frac{k_4n_2K_2^{n_2}A^{n_2-1}}{(K_2^{n_2}+A^{n_2})^2}B & -k_3-k_4S_2(A) & 0 \\ 0 & -\frac{k_6n_3K_3^{n_3}B^{n_3-1}}{(K_3^{n_3}+B^{n_3})^2}C & -k_5-k_6S_3(B) \end{pmatrix}.$$

where it is easy to see that each term is negative. For the NN and PN oscillators, only the term in the first row and first column differs and we have

$$(J_{NN})_{11}=-k_1-k_2S_1(C)-k_7\frac{(n_4+1)K_4^{n_4}A^{n_4}+A^{2n_4}}{(K_4^{n_4}+A^{n_4})^2}$$

that is always negative and

$$(J_{PN})_{11} = -k_1 - k_2 S_1(C) + k_7 \frac{n_4 K_4^{n_4} A^{n_4-1} - (n_4+1) K_4^{n_4} A^{n_4} - A^{2n_4}}{(K_4^{n_4} + A^{n_4})^2}$$

which has a positive term. Other components are given by $(J_{NN})_{ij} = (J_{PN})_{ij} = (J_{No})_{ij}$ for $(i,j) \neq (1,1)$

B Appendix: piecewise linear oscillators

Our analysis is based on the observation that each parameter K_i defines a threshold plane dividing the phase space into rectangular boxes, the so-called regulatory domains. Inside each regulatory domain, the system is linear and the analysis is straightforward.

B.1 Fixed points

The three different oscillators may admit fixed points depending on parameter values. Due to the discontinuity of the vector field, it is convenient to distinguish between two classes of fixed points: "regular" steady points and "singular" steady points. Regular steady points are defined following the well-established theory of smooth dynamical systems. Singular steady states are characterized by the fact that at least one of its components lies on a threshold and thus require a specific treatment.
Let $X_{ss} = (A_{ss}, B_{ss}, C_{ss})$ be a fixed point. The regular fixed points of the No-oscillator and the corresponding conditions of existence are given by

$$\begin{array}{l} A_{ss} = 1 \text{ for } C_{ss} < K_1 \text{ and } A_{ss} = K_2^* \text{ otherwise,} \\ B_{ss} = 1 \text{ for } A_{ss} < K_2 \text{ and } B_{ss} = K_3^* \text{ otherwise,} . \\ C_{ss} = 1 \text{ for } B_{ss} < K_3 \text{ and } C_{ss} = K_1^* \text{ otherwise.} \end{array}$$

It is easy to show that when a regular fixed point exists it is stable. Each species, A, B and C, can formally admit two different values at its resting state and thus we can distinguish between eight analytically different regular fixed points. The different possible steady states are the so-called focal points (Glass and J.S. Pasternack 1978a, 1978B; Mestl et al. 1995a,b) of the associated regulatory domain. If the focal point is inside its regulatory domain, it is a stable steady state of the system. Otherwise the system will leave the current regulatory domain and enter a new one that may have a different focal point.
The steady state X_{ss} is a singular fixed point if $0 \in \mathcal{F}(X_{ss})$ where $\mathcal{F}$ is the multi-valued function obtained when the Heaviside function of the component value that lies on its threshold is allowed to vary in $(0,1)$. For the No-oscillator, the only singular fixed point is (K_2, K_3, K_1) that exists when a solution $(\Theta_A, \Theta_B, \Theta_C) \in [0,1]^3$ can be found to the following system:

$$k_1(1-K_3) - k_2 K_3 \Theta_C = 0, k_3(1-K_3) - k_2 K_3 \Theta_A = 0, k_5(1-K_3) - k_2 K_3 \Theta_B = 0.$$

We obtain the conditions

$$K_1^* < K_1 < 1,\ K_2^* < K_2 < 1, K_3^* < K_3 < 1,$$

that (as we will show hereinafter) coincide with the conditions for oscillations. The state (K_2, K_3, K_1) is the so-called *loop characteristic state* ((68)) of the No-oscillator. We show in appendix B.4 that this singular fixed point is always unstable.
For the NN-oscillator, the values and the conditions for the existence of regular fixed points

are identical to those obtained in the No-oscillator model for the two components B_{ss} and C_{ss}. For A_{ss} we get

$$\begin{array}{rl} A_{ss}=1 & \text{for } C_{ss}<K_1 \text{ and } \quad K_4>1,\\ A_{ss}=K^*_{4,b} & \text{for } C_{ss}<K_1 \text{ and } K_4<K^*_{4,b},\\ A_{ss}=K^*_2 & \text{for } C_{ss}>K_1 \text{ and } \quad K_4>K^*_2,\\ A_{ss}=K^*_{4,a} & \text{for } C_{ss}>K_1 \text{ and } K_4<K^*_{4,a}, \end{array}$$

and, as for the No-oscillator, a regular fixed point, when it exists, is stable. Singular steady points with at least one component on a discontinuity plane may exist. As previously the *loop characteristic state* (K_2, K_3, K_1) is a singular steady state, and for $K_4 > K_2$, the conditions of existence remain the same than for the No-oscillator. If $K_4 < K_2$ conditions of existence become

$$K^*_1 < K_1 < 1,\ K^*_{4,a} < K_2 < K^*_{4,b},\ K^*_3 < K_3 < 1.$$

We show in appendix B.4 that this singular fixed point is always unstable. Moreover, an additional singular fixed point may occur on the discontinuity plane $A_{ss} = K_4$. This singular fixed point is induced by the additional self-feedback loop and defines a second loop characteristic state of the oscillator. It is easy to show that this steady state exists and is stable for $K^*_{4,b} < K_4 < 1$ and $C_{ss} < K_1$ or for $K^*_{4,a} < K_4 < 1$ and $C_{ss} > K_1$. The A-component of the steady-state, A_{ss}, can formally take five different values, so that we distinguish between twenty analytically different stable fixed points for the NN-oscillator.
For the PN-oscillator, the steady state values B_{ss} and C_{ss} and the corresponding conditions of existence remain the same. For A_{ss} we obtain the following values and conditions of existence

$$\begin{array}{rl} A_{ss}=1 & \text{for } \quad C_{ss}<K_1,\\ A_{ss}=K^*_2 & \text{for } C_{ss}>K_1 \quad \text{and} \quad K_4>K^*_2,\\ A_{ss}=K^*_4 & \text{for } C_{ss}>K_1 \quad \text{and} \quad K_4<K^*_4. \end{array}$$

The singular fixed point (K_2, K_3, K_1) when it exists is unstable (see appendix B.4). Moreover, as for the NN-oscillator, the additional self-feedback loop may induce the existence of a singular fixed point on the discontinuity plane $A_{ss} = K_4$. It is easy to show that this singular fixed point is always unstable. To sum up, the PN-oscillator has twelve different forms of stable steady states. It is worth noting that for $C_{ss} > K_1$ the two stable fixed points $A_{ss} = K^*_2$ and $A_{ss} = K^*_4$ can coexist when $K^*_2 < K_4 < K^*_4$.
To summarize, when a regular fixed point exists, it is stable. In addition, singular fixed points may exist but are unstable except the singular fixed point of the NN-oscillator satisfying $A_{ss} = K_4$. It is worth mentioning that, for a given set of parameters, a stable fixed point, when it exists, is unique except for the PN-oscillator where two stable fixed points may coexist.

B.2 Oscillations

Based on the fixed points analysis done in Appendix B.1 it is possible to derive analytically the conditions on parameters of the system for the existence of stable fixed points. These conditions are monitored by the relative location between K_i, the unity, and the associated critical value K^*_i. For instance, for the No-oscillator, it is easy to check that when $K_1 < K^*_1$, $K_2 > K^*_2$ and $K_3 < 1$, the point $(K^*_2, 1, K^*_1)$ is a stable fixed point. It is thus possible to derive exactly the sets of parameters for which there are no stable fixed points taking the complementary of the sets for which stable fixed points exist. These sets are given by (14), (15) and (16) for the three different oscillators, respectively. Since a trajectory cannot escape from the box $D = [0, 1]^3$, an oscillatory pattern exists inside the box. It is suspected that this oscillatory activity corresponds to a limit cycle (see the discussion in the section "Remarks on the oscillatory activities").
It is worth noting that (i) the limit cycles do not occur through the destabilization of a fixed point undergoing an Andronov-Hopf bifurcation and therefore we are not limited here

to small size limit cycles. (ii) Multistability between two stable fixed points exists only for the PN-oscillator: one fixed point satisfies $A_{ss} = K_4^*$ and the other $A_{ss} = K_2^*$. This is in agreement with the result stating that positive loops are responsible for multistability ((67)). (iii) When a regular fixed point exists, it is stable and only singular fixed points can be unstable. In particular, the singular fixed point (K_2, K_3, K_1) may exist for the three different oscillators and is always unstable. For the NN- and PN-oscillator an additional singular fixed point may occur on the switching surface $A = K_4$ and can be stable for the NN-oscillator whereas it is always unstable for the PN-oscillator.
If we discard bistability, the sufficient conditions for oscillations are necessary. However, it is known that such a bistability-exclusion can be broken by additional interactions that modify the cyclic nature or the monotonicity of the model and allow for multistability between a fixed point and a limit cycle, chaotic solutions or dynamics not allowed in R^2. For instance bistability may occur in two-side interaction systems, i.e., there exists j such that $\dot{x}_j = f_j(x_j, x_{j-1}, x_{j+1})$ ((48)), but not chaotic solutions (Elkhader, 1992). However, if the monotonicity property fails then chaotic solutions may appear (Di Cera et l. 1989). Moreover, a subcritical Hopf bifurcation generating bistability can be obtained in monotone negative feedback systems with a variable self-feedback loop (Hasty et al., 2002) indicating that bistability-exclusion probably requires monotonicity conditions on the self-interaction term. However, bistability often occurs in a narrow region of parameter space (see (Hasty et al., 2002) for instance) and one can expect that the probability of oscillations derived from steady state analysis constitutes a good approximation.

B.3 Calculation of $P(K_2 < K_{4,a}^*)$

We can easely check that

$$P(K_2 < K_{4,a}^*) = \frac{1}{\bar{K}_2\bar{k}_1\bar{k}_2\bar{k}_7}\left(G(\bar{k}_2+\bar{k}_7) - G(\bar{k}_7) - G(\bar{k}_2) + G(0)\right) \tag{33}$$

where

$$G(u) = \int_0^{\bar{k}_1} x(x+u)\ln(x+u)dx.$$

Integrating by parts we obtain

$$G(u) = \frac{(\bar{k}_1+u)^2}{3}(\bar{k}_1 - \frac{u}{2})\ln(\bar{k}_1+u) + \frac{u^3}{6}\ln(u) - \frac{\bar{k}_1}{36}(3\bar{k}_1 u - 6u^2 + 4\bar{k}_1^2)$$

that completes the analytical expression of $P(K_2 < K_{4,a}^*)$.
Let $r_c = k_1/k_2$ and $r_s = k_1/k_7$, analytical calculations give

$$\begin{aligned} P(K_2 < K_{4,a}^*) = \frac{1}{K}\Bigg(&\frac{1}{3} + \frac{r_s}{6r_c^2}\ln r_c + \frac{r_c}{6r_s^2}\ln r_s + \frac{r_c r_s}{6}\Big(\frac{1}{r_c}+\frac{1}{r_s}\Big)^3\ln\Big(\frac{1}{r_c}+\frac{1}{r_s}\Big) \\ &+\frac{r_s}{3}\Big(\frac{1}{r_c}+1\Big)^2\Big(\frac{1}{2}-r_c\Big)\ln\Big(1+\frac{1}{r_c}\Big) + \frac{r_c}{3}\Big(\frac{1}{r_s}+1\Big)^2\Big(\frac{1}{2}-r_s\Big)\ln\Big(1+\frac{1}{r_s}\Big) \\ &-\frac{1}{3}\Big(\frac{1}{r_c}+\frac{1}{r_s}+1\Big)^2\Big(\frac{r_s}{2}+\frac{r_c}{2}-r_c r_s\Big)\ln\Big(1+\frac{1}{r_c}+\frac{1}{r_s}\Big)\Bigg) \end{aligned}$$

B.4 Stability of the origin

For the No-oscillator, the stability of singular steady state (K_2, K_3, K_1) is determined by the stability of the origin of

$$\dot{x} = k_1(1 - K_2 - x) - k_2(x + K_2)\Theta(z),$$

$$\dot{y} = k_3(1 - K_3 - y) - k_4(y + K_3)\Theta(x),$$
$$\dot{z} = k_5(1 - K_1 - z) - k_6(z + K_1)\Theta(y).$$

which is given by the study of the trajectories of the system

$$\dot{x} = k_1(1 - K_2) - k_2K_2\Theta(z),$$
$$\dot{y} = k_3(1 - K_3) - k_4K_3\Theta(x),$$
$$\dot{z} = k_5(1 - K_1) - k_6K_1\Theta(y).$$

We define

$$\alpha_i = k_{2i-1}(1 - K_{i+1}),$$
$$\beta_i = (k_{2i-1} + k_{2i})K_{i+1} - k_{2i-1},$$

for $i = 1, 2, 3$ where we set here $K_4 = K_1$ for convenience. Conditions for the existence of a singular fixed point at the origin lead to $\alpha_i > 0$ and $\beta_i > 0$. The dynamics can be rewritten as

$$\dot{x} = \alpha_1 \quad \text{if } z < 0 \text{ and } -\beta_1 \text{ otherwise},$$
$$\dot{y} = \alpha_2 \quad \text{if } x < 0 \text{ and } -\beta_2 \text{ otherwise},$$
$$\dot{z} = \alpha_3 \quad \text{if } y < 0 \text{ and } -\beta_3 \text{ otherwise}.$$

and we have $\mathrm{sgn}(\dot{x}) = -\mathrm{sgn}(z)$, $\mathrm{sgn}(\dot{y}) = -\mathrm{sgn}(x)$ and $\mathrm{sgn}(\dot{z}) = -\mathrm{sgn}(y)$. Note that a similar system is studied in Farcot and Gouzé (2009) but with different assumptions on the parameters. Here we will show using basic calculus that the "local" system is unstable.
The trajectories make revolutions around the origin and pass many times into the plane $x = 0$, intersecting it for $y > 0$ (and $z < 0$) and for $y < 0$ (and $z > 0$) for one revolution. After possibly a transient, the sign of the components defining the trajectory will follow the cycle $(+,+,-) \to (+,-,-) \to (+,-,+) \to (-,-,+) \to (-,+,+) \to (-,+,-)$ (see Fig. 6 where 1 corresponds to + and 0 to −).
The trajectory of the system defines a mapping of the half plane P_0 ($x_0 = 0$, $y_0 > 0$, $z_0 < 0$) into itself. The solution with initial value $x_0 = 0$, $y_0 > 0$, $z_0 < 0$ lies first in the region (110) i.e. ($x > 0$, $y > 0$, $z < 0$), where the solution has the form

$$x(t) = \alpha_1 t, \quad y(t) = y_0 - \beta_2 t, \quad z(t) = z_0 - \beta_3 t.$$

The trajectory intersects the plane $y = 0$ at time $t_a = y_0/\beta_2$ at the point

$$x_a = \alpha_1/\beta_2 y_0, \quad y_a = 0, \quad z_a = z_0 - \beta_3/\beta_2 y_0,$$

and enters into the domain 100. Using similar arguments, we compute the different reaching times, $t_a, \ldots, t_f$, of the different regions (101, 001, 011, 010 and 110, respectively) together with the corresponding intersection points. We find that from the point $x_0 = 0$, $y_0 > 0$, $z_0 < 0$ in P_0 the trajectory first goes back into P_0 at the point $x_f = 0$, y_f, z_f where

$$\begin{pmatrix} y_f \\ z_f \end{pmatrix} = \begin{pmatrix} a_{11} & a_{12} \\ a_{21} & a_{22} \end{pmatrix} \begin{pmatrix} y_0 \\ z_0 \end{pmatrix} \tag{34}$$

with

$$a_{11} = 3 + u_1 + u_2 + u_3 + u_1u_2 + u_1u_3 + u_2u_3 + u_1u_2u_3 + \frac{1}{u_1} + \frac{1}{u_3} + \frac{1}{u_1u_3},$$
$$a_{12} = -\frac{\beta_2}{\beta_3}\left(2 + u_1 + u_2 + u_1u_2 + \frac{1}{u_1} + \frac{1}{u_3} + \frac{1}{u_1u_3}\right),$$
$$a_{21} = -\frac{\beta_3}{\beta_2}\left(1 + u_3 + \frac{u_3}{u_2} + \frac{2}{u_2} + \frac{1}{u_1u_2} + \frac{1}{u_2u_3} + \frac{1}{u_1u_2u_3}\right),$$
$$a_{22} = 1 + \frac{1}{u_2} + \frac{1}{u_1u_2} + \frac{1}{u_2u_3} + \frac{1}{u_1u_2u_3},$$

where we set $u_i = \alpha_i/\beta_i$.
Equation (34) defines a 2D-linear mapping. Let λ_1 and λ_2 be the two associated eigenvalues. Since we have $|\lambda_1|+|\lambda_2| \geq |\lambda_1+\lambda_2| = |a_{11}+a_{22}| > 4$ then at least one eigenvalue is greater than 1 in absolute value. Therefore, the origin is unstable. Numerical investigations suggest than one eigenvalue is large whereas the other is less than one , in absolute value, indicating a saddle configuration and the existence of a stable manifold associated with the origin.
For the two others oscillators, the NN-oscillator and the PN-oscillator, the situation remains the same for $K_4 > K_2$. When $K_4 < K_2$ we define $\alpha_{1,NN} = \alpha_1 - k_7K_2$ and $\beta_{1,NN} = \beta_1 + k_7K_2$ for the NN-oscillator and $\alpha_{1,PN} = \alpha_1 + k_7(1-K_2)$ and $\beta_{1,PN} = \beta_1 - k_7(1-K_2)$ for the PN-oscillator. Conditions for the existence of the singular fixed point (K_2, K_3, K_1) give $\alpha_{1,NN} > 0$, $\beta_{1,NN} > 0$ and $\alpha_{1,PN} > 0$, $\beta_{1,PN} > 0$. Study of stability proceeds along the same lines than for the No-oscillator and we show that the origin is unstable.

C The random parameter sets

For the numerical simulation of the smooth oscillators, we used the same parameter distributions as in (Tsai et al. 2008). All parameters are dimensionless and (H) holds (see (22)) with:

- $K = 4$, i.e., we used $K_i \sim U(0, 4)$, $i = 1, 2, 3, 4$,
- $k = 10$, i.e., we used $k_1, k_3 \sim U(0, 10)$,
- $k_c = 1000$, i.e., we used $k_2, k_4, k_6 \sim U(0, 1000)$

except for k_5 that has been fixed to 1. For the NN-oscillator and PN-oscillator, we used $k_7 \sim U(0, 100)$. Each Hill coefficient follows an uniform distribution over $(1, 4)$.

References

1. V. Acary, H. de Jong, and B. Brogliato, (2014), Numerical simulation of piecewise-linear models of gene regulatory networks using complementarity systems, Physica D 269, 103-119.
2. D. Angeli, J.E. Ferrell, and E.D. Sontag, (2004), Detection of multistability, bifurcations, and hysteresis in a large class of biological positive-feedback systems, Proc. Natl. Acad. Sci. USA 101, 1822-1827.
3. F. Boulier, M. Lefranc, F. Lemaire,P.-E. Morant and A. Ürgüplü (2007) in H. Anai and K. Horimoto and T. Kutsia (Ed.), On proving the absence of oscillations in models of genetic circuits, Proceedings of Algebraic Biology, LNCS 4545, 66-80.
4. O. Buse, A. Kuznetsov, and R. Pérez, (2009), Existence of limit cycles in the repressilator equations, Int. J. Bifurcat. Chaos 19, 4097-4106.
5. O. Buse, R. Pérez, and A. Kuznetsov, (2010), Dynamical properties of the repressilator model, Phys. Rev. E 81, doi: 10.1103/PhysRevE.81.066206.
6. J.L. Cherry and F.R. Adler, (2000), How to make a biological switch, J. Theor. Biol. 203, 117-113.
7. A. Ciliberto, B. Novak, and J.J. Tyson, (2005), Steady states and oscillations in the p53/Mdm2 network, Cell Cycle 4, 488-493.
8. O. Cinquin and J. Demongeot, (2002), Positive and negative feedback: striking a balance between necessary antagonists, J. Theor. Biol. 216, 229-241.
9. H. de Jong, J. Geiselmann, C. Hernandez, and M. Page, (2003), Genetic network analyzer: qualitative simulation of genetic regulatory networks, Bioinformatics 19, 336-344.
10. J. Demongeot, N. Glade, and L. Forest, (2007a), Liénard systems and potential-Hamiltonian decomposition I - Methodology, C. R. Acad. Sci. Paris - Ser. I - Mathematics 344, 121-126.
11. J. Demongeot, N. Glade, and L. Forest, (2007b), Liénard systems and potential-Hamiltonian decomposition II - Algorithm, C. R. Acad. Sci. Paris, Ser. I- Mathematics 344, 191-194.

12. E. Di Cera, P.E. Phillipson, and J. Wyman, (1989), Limit-cycle oscillations and chaos in reaction networks subject to conservation of mass, Proc. Natl. Acad. Sci. USA 86, 142-146.
13. A. Dokoumetzidis, A. Iliadis, and P. Macheras, (2001), Nonlinear dynamics and chaos theory: concepts and applications relevant to pharmacodynamics, Pharm. Res. 18, 415-426.
14. M. Domijan and E. Pécou, (2012), The interaction graph structure of mass-action reaction networks, J. Math. Biol. 65, 375-402.
15. A. S. Elkhader, (1992), A result on a feedback system of ordinary differential equations, J. Dyn. Differ. Equ. 4, 399-418.
16. M.B. Elowitz and S. Leibler, (2000), A synthetic oscillatory network of transcriptional regulators, Nature 403, 335-338.
17. D.R. Falkenburg, Existence of limit cycles in a non linear dynamic system with random parameters, (1979), WSC '79 Proceedings of the 11th conference on Winter simulation 1, 159-164.
18. E. Farcot and J. L. Gouzé, (2009), Periodic solutions of piecewise affine gene network models with non uniform decay rates: the case of a negative feedback loop, Acta Biotheoretica 57, 429-455.
19. E. Farcot and J. L. Gouzé, (2010), Limit cycles in piecewise-affine gene network models with multiple interaction loops, International Journal of Systems Science 41, 119-130.
20. J.E. Ferrell, (2002), Self-perpetuating states in signal transduction: positive feedback, double-negative feedback and bistability, Curr. Opin. Chem. Biol. 6, 140-148.
21. J.E. Ferrell, T.Y. Tsai, and Q. Yang, (2011), Modeling the cell cycle: why do certain circuits oscillate?, Cell 144, 874-885.
22. A.F. Filippov (1988) Differential equations with discontinuous righthand sides, Kluwer Academic Publishers, Dordrecht, the Netherlands.
23. A. Fraser and J. Tiwari, (1974), Genetic feedback-repression. II. Cyclic genetic systems, J. Theor. Biol. 47, 397-412.
24. T.S. Gardner, C.R. Cantor, and J.J. Collins, (2000), Construction of a genetic toggle switch in Escherichia coli, Nature 403, 339-342.
25. T. Gedeon (1998) Cyclic Feedback Systems, Mem. Am. Math. Soc. 134 (637).
26. T. Gedeon and K. Mischaikow, (1995), Structure of global attractor of cyclic feedback systems, J. Dyn. Differ. Equ. 7, 141-190.
27. L. Glass and S.A. Kaufman, (1973), The logical analysis of continuous, non-linear biochemical control networks, J. Theor. Biol. 39, 103-129.
28. L. Glass and J.S. Pasternack, (1978a), Prediction of limit cycles in mathematical models of biological oscillations, B. Math. Biol. 40, 27-44.
29. L. Glass and J.S. Pasternack, (1978b), Stable oscillations in mathematical models of biological control systems, J. Math. Biol. 6, 207-223.
30. A. Goldbeter, (1991), A minimal cascade model for the mitotic oscillator involving cyclin and cdc2 kinase, Proc. Natl. Acad. Sci. USA 88, 9107-9111.
31. A. Goldbeter, (2002), Computational approaches to cellular rhythms, Nature 420, 238-245.
32. J.L. Gouzé, (1998), Positive and negative circuits in dynamical systems, J. Biol. Sys. 6, 11-15.
33. J.L. Gouzé and T. Sari, (2002), A class of piecewise linear differential equations arising in biological models, Dynam. Syst. 17, 299-316.
34. S. Grandison and R.J. Morris, (2008), Biological pathway kinetic rate constants are scale-invariant, Bioinformatics 24, 741-743.
35. J. Griffith, (1968), Mathematics of cellular control processes. I. Negative feedback to one gene, J. Theor. Biol. 20, 202-208.
36. S.L. Harris and A.J. Levine, (2005), The p53 pathway: positive and negative feedback loops, Oncogene 24, 2899-2908.
37. S.P. Hastings, (1977), On the uniqueness and global asymptotic stability of periodic solutions for a third order system, Rocky Mt. J. Math. 7, 513-538.
38. S. Hastings, J. Tyson, and D. Webster, (1977) Existence of periodic solutions for negative feedback cellular control systems, J. Differ. Equations 25, 39-64.

39. J. Hasty, M. Dolnik, V. Rottschäfer, and J.J. Collins, (2002), Synthetic gene network for entraining and amplifying cellular oscillations, Phys. Rev. Lett. 88, 148101.
40. H. Hirata, S. Yoshiura, T. Ohtsuka, Y. Bessho, T. Harada, K. Yoshikawa, and R. Kageyama, (2002), Oscillatory expression of the bHLH factor Hes1 regulated by a negative feedback loop, Science 298, 840-843.
41. M.W. Hirsch, (1982), Systems of differential equations which are competitive and cooperative. I: Limit sets, SIAM J. Math. Anal. 13, 167-179.
42. M.W. Hirsch, (1985), Systems of differential equations that are competitive and cooperative. II: Convergence almost everywhere, SIAM J. Math. Anal. 16, 425-439.
43. G. Hornung and N. Barkai, (2008), Noise propagation and signaling sensitivity in biological networks: a role for positive feedback, PLoS Comput. Biol. 4, doi: 10.1371/journal.pcbi.0040008.
44. L. Ironi, L. Panzeri, E. Plahte, and V. Simoncini, (2011), Dynamics of actively regulated gene networks, Physica D 240, 779-794.
45. M. Kaufman, C. Soulé, and R. Thomas, (2007), A new necessary condition on interaction graphs for multistationarity, J. Theor. Biol. 248, 675-685.
46. J. Keener and J. Sneyd (1998) Mathematical Physiology. I: Cellular Physiology, Interdisciplinary Applied Mathematics 8, Springer.
47. F. López-Caamal, R. H. Middleton, and H.J. Huber, (2013), Equilibria and stability for a class of positive feedback loops: mathematical analysis and its application to caspase-dependent apoptosis, J. Math. Biol. 68, 609-645.
48. W. Li, S. Krishna, S. Pigolotti, N. Mitarai, and M.H. Jensen, (2012), Switching between oscillations and homeostasis in competing negative and positive feedback motifs, J. Theor. Biol. 307, 205-210.
49. J. Lin and P. B. Kahn, (1977), Limit cycles in random environments, SIAM J. Appl. Math. 32, 260-291.
50. L. Lu and R. Edwards, (2010), Structural principles for periodic orbits in Glass networks, J. Math. Biol. 60, 513-541.
51. A. Machina, R. Edwards, and P. van den Driessche, (2013), Singular dynamics in gene network models, SIAM J. App. Dyn. Syst. 12, 95-125.
52. J. Mallet-Paret and H.L. Smith, (1990), The Poincaré-Bendixson theorem for monotone cyclic feedback systems, J. Dyn. Differ. Equ. 2,367-421.
53. K. Matsuoka, (1985), Sustained oscillations generated by mutually inhibiting neurons with adaptation, Biol. Cyber. 52, 367-376.
54. H.P. McKean, (1970), Nagumo's equation, Adv. Math. 4, 209-223.
55. T. Mestl, E. Plahte, and S.W. Omholt, (1995a), A Mathematical framework for describing and analysing gene regulatory netwoks, J. Theor. Biol. 176, 291-300.
56. T. Mestl, E. Plahte, and S. W. Omholt, (1995b), Periodic solutions in systems of piecewise-linear differential equations, Dynam. Stabil. Syst. 10, 179-193.
57. M. Mincheva, (2011), Oscillations in biochemical reaction networks arising from pairs of subnetworks, Bull. Math. Biol. 73, 2277-2304.
58. S. Müller, J. Hofbauer, L. Endler, C. Flamm, S. Widder, and P. Schuster, (2006), A generalized model of the repressilator, J. Math. Biol. 53, 905-937.
59. S. Pigolotti, S. Krishna, and M.H. Jensen, (2007), Oscillation patterns in negative feedback loops, Proc. Natl. Acad. Sci. USA 104, 6533-6537.
60. E. Plahte and S. Kjoglum, (2005), Analysis and generic properties of gene regulatory networks with graded response functions, Physica D 201, 150-176.
61. E. Plahte, T. Mestl, and W. S. Omholt, (1995), Feedback loops, stability and multistationarity in dynamical systems, J. Biol. Sys. 3, 409-413.
62. O. Purcell, N.J. Savery, C.S. Grierson, and M. di Bernardo, (2010), A comparative analysis of synthetic genetic oscillators, J. R. Soc. Interface 7, 1503-1524.
63. Adrien Richard and Jean-Paul Comet, (2011), Stable periodicity and negative circuits in differential systems, J. Math. Biol. 63, 593-600.
64. H.L. Smith, (1986), Periodic orbits of competitive and cooperative systems, J. Diff. Equations 65, 361-373.
65. H. Smith, (1987), Oscillations and multiple steady states in a cyclic gene model with repression, J. Math. Biol. 25, 169-190.

66. E.H. Snoussi, (1989), Qualitative dynamics of piecewise-linear differential equations, Dyn. Stab. Syst. 4, 189-207.
67. E.H. Snoussi, (1998), Necessary conditions for multistationarity and stable periodicity, J. Biol. Syst. 6, 3-9.
68. E.H. Snoussi and R. Thomas, (1993), Logical identification of all steady states: the concept of feedback loop characteristic states, Bull. Math. Biol. 55, 973-991.
69. N. Strelkowa and M. Barahona, (2010), Switchable genetic oscillator operating in quasi-stable model, J. R. Soc. Interface 7, 1071-1082.
70. J. Stricker, S. Cookson, M.R. Bennett, W.H. Mather, L.S. Tsimring, and J. Hasty, (2008), A fast, robust and tunable synthetic gene oscillator, Nature 456, 516-519.
71. R. Thomas, (1981), On the relation between the logical structure of systems and their ability to generate multiple steady states or sustained oscillations, Springer Ser. Synergetics 9, 180-193.
72. T.Y.C. Tsai, Y.S. Choi, W. Ma, J.R. Pomerening, C. Tang, and J.E. Jr Ferrell, (2008), Robust, tunable biological oscillations from interlinked positive and negative feedback loops, Science 321, 126-129.
73. J.J. Tyson, (1975), On the existence of oscillatory solutions in negative feedback cellular control processes, J. Math. Biol. 1, 311-315.
74. J.J. Walker, F. Spiga, E. Waite, Z. Zhao, Y. Kershaw, J.R. Terry, and S.L. Lightman, (2012), The origin of glucocorticoid hormone oscillations, PLoS Biol. 10,doi: 10.1371/journal.pbio.1001341.
75. A. Weber, T. Sturm, and E.O. Abdel-Rahman, (2011), Algorithmic global criteria for excluding oscillations, Bull. Math. Biol. 73, 899-916.